Characterization and Optimization of Organoclay-poly(melamine-co-formaldehyde)-methylated Solution Impregnated Pulai (*Alstonia* spp.) Wood Using Response Surface Methodology

Perry Law Nyuk Khui,[a] Md. Rezaur Rahman,[a,*] Hafizah binti Abdul Halim Yun,[a] Durul Huda,[b] Sinin Hamdan,[a] Muhammad Khusairy Bin Bakri,[a] Mohammad Mahbubul Matin,[c] Kuok King Kuok,[d] Chin Mei Yun, [d] Abdullah S. Al-Bogami,[e] Khalid A. Alamry,[f] and Mohammed M. Rahman [f,*]

Significant effects of organoclay and poly(melamine-co-formaldehyde)-methylated (PMFM) impregnation on the mechanical, morphological, and thermal characteristics of raw pulai wood were investigated in this work. The material's modulus of elasticity (MOE) as well as the maximum compression force (MCF) of the impregnated organoclay/PMFM pulai wood samples were optimized using a designed experiment. The MOE and MCF models had R^2 values of 0.9228 and 0.8340, respectively. After the impregnation of organoclay/PMFM pulai wood samples, the MOE and MCF increased considerably, indicating that the pulai wood's mechanical characteristics had improved. The compositional analysis verified the polymerization and dispersion of organoclay and PMFM. Using Fourier transform infrared spectroscopy, reduction in the hydroxyl groups was detected. The impregnated organoclay/PMFM pulai wood samples had successfully filled the pores and cell cavities, as seen by scanning electron microscopy. The thermal stability of the impregnated organoclay/PMFM pulai wood samples was better than that of the raw pulai wood, with a higher glass transition temperature as determined by differential scanning calorimetry. The thermogravimetric study revealed that the impregnated organoclay/PMFM pulai wood samples had higher decomposition temperatures than the raw pulai wood sample.

DOI: 10.15376/biores.17.2.2780-2809

Keywords: Wood; Impregnation; Characterization; Treatment; Chemical; Response surface methodology

Contact information: a: Faculty of Engineering, Universiti Malaysia Sarawak, Jalan Datuk Mohammad Musa, 94300, Kota Samarahan, Sarawak, Malaysia; b: Department of Mechanical Engineering and Product Design Engineering, Swinburne University of Technology, 3122, Hawthorn, Victoria, Australia; c: Department of Chemistry, University of Chittagong, Chittagong, 4331, Bangladesh; and d: Faculty of Engineering, Computing and Science, Swinburne University of Technology Sarawak Campus, Jalan Simpang Tiga, 93250, Kuching, Sarawak, Malaysia; e: Department of Chemistry, College of Sciences, University of Jeddah, Jeddah 21589, P.O. Box 80327, Saudi Arabia; f: Department of Chemistry, Faculty of Science, King Abdulaziz University, Jeddah 21589, P.O. Box 80203, Saudi Arabia;
** Corresponding author: rmrezaur@unimas.my*

INTRODUCTION

Alstonia spp. (Apocynaceae) wood is called mengalang, pelai, or pulai in Southeast Asia in general, especially in Malaysia and Indonesia (Wong 2002; How and Nordahlia 2018; Mery *et al*. 2019; Oktavia *et al*. 2020). A few of its known species are *A. angustiloba*,

A. macrophylla, *A. pneumatophore*, *A. scholaris*, and *A. spatulata*. Despite the high moisture content of the wood, it is often used for household objects, carvings, and sculptures (Oktavia *et al*. 2020). Carving, crates and packing boxes, frames, fret work, match boxes and splints, pattern making, plywood, picture frames, pencil, and toothpicks are all possible uses for the wood. It has also been used to make wooden clogs and disposable chopsticks with great success. Basong, the root wood of *A. spatulata* and *A. pneumatophora*, is incredibly light, weighing just 50 to 80 kg/m^3 air dried, and has been used to make pith-helmets (Wong 2002).

The sapwood is undifferentiated from the heartwood, which ranges in color from cream to light yellow. The wood is listed as a light hardwood with an air-dry density of 210 to 500 kg/m^3 (H'ng *et al*. 2010; How and Nordahlia 2018; How and Sik 2020). Pulai is classed as non-durable based on a standard burial test of untreated specimens with dimensions of 50 mm x 50 mm x 600 mm (Foxworthy and Woolley 1930). Within 6 months, all 21 parts of the specimens tested were destroyed (Foxworthy and Woolley 1930). On the wood, both fungus and insect infestations were widespread. Preservatives are thus a simple option that may be applied to the wood. The use of pulai wood grain is straight to shallowly interlaced, and the texture is relatively fine to coarse (Monachino 1949). Pulai wood matures fast, with less cupping, bending, twisting, and end-checking than other woods. Powder-post beetle and sap stain fungus are both known to damage the wood. Air drying takes around 1.5 months for 13-mm-thick boards and 2.5 months for 38-mm-thick boards. It is suggested to use the Kiln Schedule J method for drying (Bond and Espinoza 2016). Pulai wood shrinkage is substantial, particularly in the radial direction, where it averages 2.3%, while tangential shrinkage averages 2.8% (Malaysian Timber Corporation 1982).

Due to its susceptibility to fungi and bacteria, it is important to treat the wood to reduce these problems. Other procedures, such as wood modification, pulping, bonding, and coating technologies, may rely on the treatability of wood (Torgovnikov and Vinden 2009; Biziks *et al.* 2019). A significant penetration of reaction agents into wood is required to ensure a proper bulk chemical modification; otherwise, due to a non-uniform dispersion of the agent, the inner regions of wood may not be suitably changed (Homan and Jorissen 2004).

Poor penetration of finishes into wood can have a detrimental impact on coating performance of solvent- and water-borne finishes on wood because coating adherence to the wood surface benefits to some extent from penetration (De Meijer and Militz 1998). Mader *et al.* (2011) presented an excellent literature study on coating penetration into wood. Kamke and Lee (2007) also published an excellent scientific review study on adhesive penetration in wood, focusing on the adhesive bond performance of wood-based composites. To achieve effective bond performance, a specific amount of adhesive penetration into the wood is required throughout the composites manufacturing process (Kamke and Lee 2007).

A model was made based on Design Expert 11 software, which was used to analyze the response surface methodology (RSM) of the sample. The model created was also used to predict the compression strength of the actual impregnated sample. The study on its compression strength properties was considered with changes of the parameters, which were changed accordingly to its weight percentage of the PMFM, weight percentage of the organoclay, and the duration of impregnation.

EXPERIMENTAL

Materials

Pulai wood was cut from the local forest from Kuching, Sarawak, Malaysia. Organoclay CLAYTONE®EM with CAS Number 14808-60-7 was obtained from BYK Additives Inc. (Wesel, Germany). The size of the organoclay is around 40-100 mesh. Poly(melamine-co-formaldehyde)-methylated (PMFM), solution with product number 418560-250ML and CAS Number 68002-20-0, was obtained from Sigma-Aldrich (Darmstadt, Germany). Dichloromethane (AR Grade, 2.5 L) with product number A709-2.6LGL was obtained from Ajax Finechem (UNIVAR, Victoria, Australia). Dichloromethane was used in the actual sample as a medium dilution solvent to allow the chemical to be impregnated in the wood samples.

Sample Preparation

To prepare the samples, the Pulai wood was cut into similar rectangular cuboid size, with the fiber direction towards the longitudinal axis, as shown in Fig. 1(a).

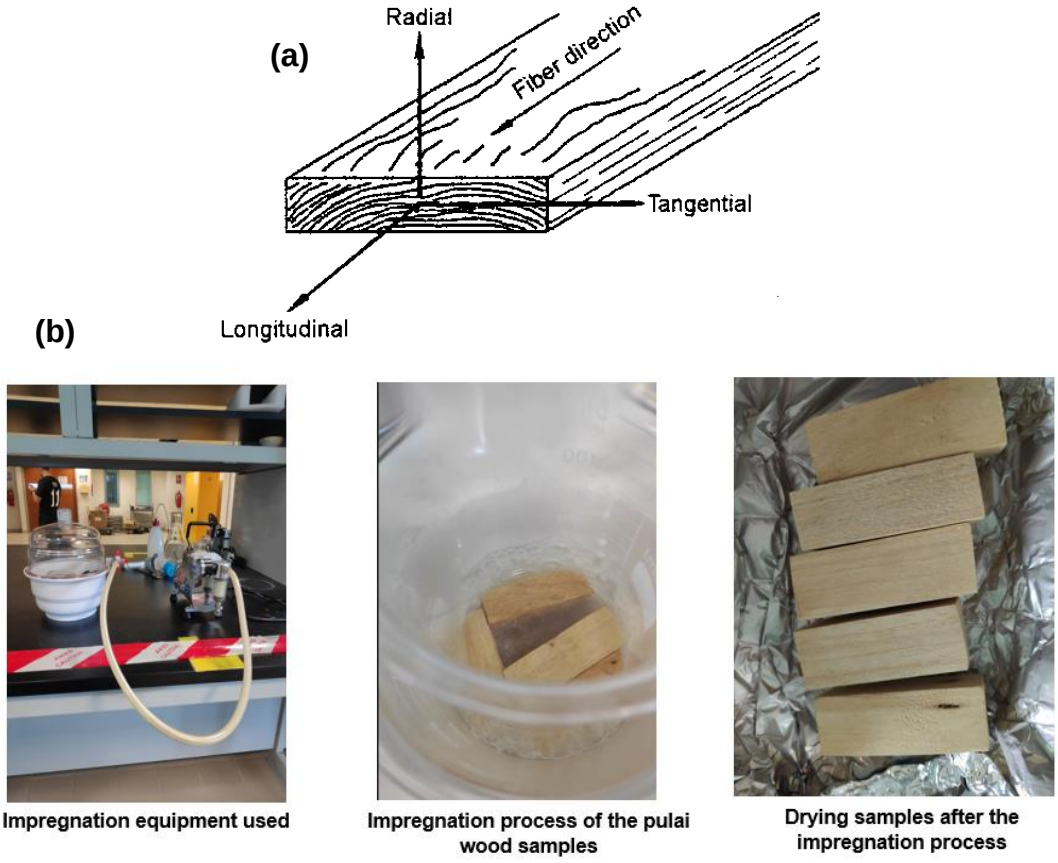

Fig. 1. (a) Three principial axis of wood with respect to fiber direction and growth rings; (b) the apparatus, impregnation process, and drying samples

The untreated samples were placed in a forced air convection oven (IMPACT Ltd., Southampton, UK), Model P12VSD) for 24 h at 70 °C for conditioning and drying. This reduced or eliminated the presence of moisture in the untreated samples. The oven-dried samples were immersed and prepared by adding the different amounts of organoclay and

PMFM, which was diluted with dichloromethane. The raw samples and the diluted solution were transferred into a concealed impregnation chamber and were impregnated at different durations. Once the impregnation process was completed, the impregnated samples were cleaned and wrapped with aluminum foil and placed into an oven at 70 °C for 48 h, to allow polymerization, curing process, and cross linkage between PMFM and organoclay to occur. The final impregnated samples were unwrapped for mechanical testing and characterization.

Design of Experiment (DOE)

Impregnated samples were prepared in accordance with a design of experiment (DOE). This DOE was conducted using "Design Expert 11 software (Stat-Ease, Minneapolis, MN, USA) with three main variables: A: duration (min), B: PMFM (wt%), and C: organoclay (wt%). Table 1 shows the range of variables at a low level of −1 and a high level of +1. The experiment was made up of 20 runs with an average of five replicates for each sample, details are presented in Table 2. Statistical analysis of the process was performed to evaluate the analysis of variance (ANOVA).

Table 1. Variables Used in the DOE

Parameters	Levels	
	Low (-1)	High (+1)
A: Time (min)	15.00	120.00
B: Poly(melamine-co-formaldehyde)-methylated Solution (wt%)	1.00	10.00
C: Organoclay (wt%)	0.50	2.00

Table 2. DOE from Design Expert 11

Standard (Std)	Run	A: Time (min)	B: Poly(melamine-co-formaldehyde) Methylated Solution (wt%)	C: Organoclay (wt%)
7	1	15.0	10.0	2.00
17	2	67.5	5.5	1.25
10	3	120.0	5.5	1.25
19	4	67.5	5.5	1.25
20	5	67.5	5.5	1.25
11	6	67.5	1.0	1.25
2	7	120.0	1.0	0.50
5	8	15.0	1.0	2.00
13	9	67.5	5.5	0.50
16	10	67.5	5.5	1.25
3	11	15.0	10.0	0.50
18	12	67.5	5.5	1.25
6	13	120.0	1.0	2.00
8	14	120.0	10.0	2.00
12	15	67.5	10.0	1.25
15	16	67.5	5.5	1.25
14	17	67.5	5.5	2.00
1	18	15.0	1.0	0.50
9	19	15.0	5.5	1.25
4	20	120.0	10.0	0.50

The experiments were run to minimize experimental errors. The relationship between the independent variables and their responses, *i.e.*, higher modulus of elasticity (MOE) and maximum compressive force (MCF) were fitted to a quadratic model, as expressed in Formula 1,

$$y = \beta + \beta A + \beta B + \beta C + \beta AB - \beta AC + \beta BC + \beta A^2 - \beta B^2 - \beta C^2 \quad (1)$$

where y is the response, and β is the constant term.

Characterization of the Experimental Samples

From the results obtained in Table 2 from the DOE, which involved the test with a higher MOE and MCF, some samples of the impregnated organoclay/PMFM pulai wood samples as presented in Table 3 were characterized and compared with the raw samples to study the effects of the impregnation.

Table 3. Selected Runs for Characterizations for Actual Testing

Samples Label	A: Time (min)	B: Poly(melamine-co-formaldehyde) Methylated Solution (wt%)	C: Organoclay (wt%)	MOE (MPa)	MCF (kN)
Raw	-	-	-	-	-
A1	120.00	10.00	0.50	4.96	12.47
A2	15.00	10.00	0.50	6.16	13.73
A3	15.00	1.00	0.50	5.76	13.04
A4	120.00	1.00	0.50	6.71	12.70
A5	67.50	5.50	0.50	10.04	13.71
B1	67.50	10.0	1.25	5.78	9.72
B2	67.50	5.50	1.25	9.39	15.19
B3	120.00	5.50	1.25	8.28	14.23
B4	67.50	1.00	1.25	6.60	13.63
B5	15.0	5.50	1.25	11.11	14.00
C1	120.00	10.00	2.00	4.02	9.14
C2	15.00	10.00	2.00	7.05	10.47
C3	67.50	5.50	2.00	6.99	11.70
C4	120.00	1.00	2.00	4.02	9.144
C5	15.00	1.00	2.00	4.68	9.10

Compression test

A universal testing machine (MSC-5/500, Shimadzu Corporation, Kyoto, Japan) was used for compression testing. An average of 5 samples for each impregnated organoclay/PMFM pulai wood samples was obtained and tabulated according to Table 3. The test was performed according to ASTM D3501-05 (2018).

Fourier transform infrared spectroscopy

Shimadzu Corporation's (Kyoto, Japan) FTIR "IRAffinity-1" spectroscope was utilized. The molecular bond structures and functional groups of the impregnated organoclay/PMFM pulai wood samples were identified using IR spectra bands ranging from 4000 to 400 cm^{-1}. The FTIR spectrum was plotted using "IR solution" software (IR solution, Shimadzu, Tokyo, Japan) based on ASTM E168-16 (2016) and ASTM E1252-98 (2021) standards.

Differential scanning calorimetry (DSC)

For DSC measurements, a DSC Q10 (TA Instruments, New Castle, DE, USA) thermal system with a sealed aluminum capsule was used. Each set of data represents the average of five different runs. The specimen was 4 to 4.5 mg and heated at a constant rate of 10 °C/min, while the scanning temperature was adjusted between 30 and 600 °C. The samples' crystallization and melting temperatures were determined to be in compliance with ASTM D3418-15 (2015) and ASTM E1269-11 (2018) requirements, respectively.

Scanning electron microscopy (SEM) with energy dispersive spectroscopy (EDS/EDX)

Hitachi Analytical's Tabletop scanning electron microscope (SEM) model TM-3030 (Hitachi High-Technologies Europe GmbH, Krefeld, Germany) was used to capture the morphological images of raw and impregnated organoclay/PMFM pulai wood samples. Field emission with a 15 kV accelerating voltage was used to gather images of the surface of samples. The tests were conducted in accordance with ASTM E2015-04 (2014), with a magnification of 800x.

Thermogravimetric analysis (TGA)

A Pyris™ 1 TGA from Perkin Elmer Inc. (Waltham, MA, USA) machine was used for the thermogravimetric analysis (TGA) measurements. Analyses were performed at temperatures ranging from 30 to 600 °C with a nitrogen flow rate of 20 mL/min. During these tests, a heating rate of 20 °C/min was maintained. The test was performed in line with ASTM E1131-20 (2020).

RESULTS AND DISCUSSION

Statistical Analysis of MOE and MCF by ANOVA

The ANOVA is a crucial statistical method for deducing inferences from solutions and analyzing experimental data. The benefits given by this technique were investigated to evaluate the interactions and effects of chemical treatment on the mechanical characteristics of impregnated organoclay/PMFM pulai wood samples. The Fisher's variance F-value was calculated using the sum of squares and mean squares in Table 4, which is a measure of data variation around the mean. In contrast, the P-value indicates how important a parameter might become. Therefore, the early hypothesis can be rejected because a parameter with a P-value greater than 0.10 was not insignificant. When the P-value is less than 0.05, the model terms are considered significant. Time, PMFM, and organoclay all had substantial impacts on the samples, as seen in Table 4. The MOE was also affected by interactions between time and PMFM, PMFM and organoclay, and time and organoclay. As indicated in Table 5, comparable interactions were detected on the MCF's resulting characteristics. The MOE had an R^2 value of 0.9228, which was relatively close to 1, indicating that the model was valid, with an adjusted R^2 value of 0.8534 within a 0.2 difference, whereas the R^2 indicates the quality of the experimental data used in building the model. Similar results were also obtained by Jiang *et al.* (2020) and Adamu *et al.* (2020, 2021).

Table 4. The ANOVA Results for MOE

Source	Sum of Squares	Mean Squares	F Value	P-value Prob > F
Model	73.10	8.12	13.29	0.0002
A-Time	1.98	1.98	3.23	0.1024
B-Poly(melamine-co-formaldehyde)-methylated Solution	0.045	0.45	0.73	0.4122
C-Organoclay	2.08	2.08	3.40	0.0950
AB	5.84	5.84	9.55	0.0115
AC	0.16	0.16	0.26	0.6225
BC	0.25	0.25	0.41	0.5381
A^2	0.31	0.31	0.51	0.4912
B^2	27.63	27.63	45.21	<0.0001
C^2	1.97	1.97	3.22	0.1030
R^2 = 0.9228				
Adjusted R^2 = 0.8534				
Predicted R^2 = 0.8996				

Table 5. The ANOVA Results for MCF

Source	Sum of Squares	Mean Squares	F Value	P-value Prob > F
Model	69.04	7.67	5.58	0.0064
A-Time	0.56	0.56	0.40	0.5391
B-Poly(melamine-co-formaldehyde)-methylated Solution	5.00	5.00	3.64	0.0856
C-Organoclay	12.16	12.26	8.93	0.0136
AB	6.64	6.64	4.83	0.0526
AC	3.53	3.53	2.57	0.1401
BC	2.11	2.11	1.53	0.2440
A^2	0.22	0,22	0.16	0.6975
B^2	12.78	12.78	9.30	0.0123
C^2	3.48	3.48	2.53	0.1425
R^2 = 0.8340				
Adjusted R^2 = 0.6847				
Predicted R^2 = -0.7277				

The R^2, adjusted R^2, and predicted R^2 for the MCF were 0.8340, 0.0687, and minus 0.7277, respectively. The MCF values are similarly comparable to earlier values of MOE. Equations 1 and 2 offer model equations for the MOE and MCF based on coded factors of +1 for the high level and 1 for the low level, represented as:

$$MOE = 9.38 - 0.45A - 0.21B - 0.46C - 0.85AB - 0.14AC + 0.18BC + 0.34A^2 - 3.17B^2 - 0.85C^2 \quad (1)$$

$$MCF = 14.64 + 0.24A - 0.71B - 1.11C - 0.91AB + 0.66AC - 0.51BC + 0.28A^2 - 2.16B^2 - 1.13C^2 \quad (2)$$

Table 6 shows that the predictions from the model were extremely similar to the actual values with very low residuals (Adamu *et al*. 2020, 2021; Jiang *et al*. 2020). Figures 2a and 2b show the plots for the MOE and MCF of the predicted *versus* actual. As a result of the minimal variation, the model appears to be capable of accurately predicting the mechanical characteristics of impregnated organoclay/PMFM pulai wood samples.

Table 6. Comparison of the Actual Values and Predicted Values

Run	A: Time (min)	B: Poly(melamine-co-formaldehyde)-methylated Solution (wt%)	C: Organ-oclay (wt%)	Actual Values		Predicted Values		Residual		Re-marks
				MOE	MCF	MOE	MCF	MOE	MCF	
1	15.0	10.0	2.00	7.05	10.47	6.65	9.33	0.396	1.14	
2	67.5	5.5	1.25	9.39	15.19	9.38	14.64	0.013	0.543	
3	120.0	5.5	1.25	8.28	14.23	9.27	15.16	-0.989	-0.935	
4	67.5	5.5	1.25	9.39	15.19	9.38	14.64	0.013	0.543	
5	67.5	5.5	1.25	9.39	15.19	9.38	14.64	0.013	0.543	
6	67.5	1.0	1.25	6.60	13.63	6.42	13.20	0.179	0.430	
7	120.0	1.0	0.50	6.71	12.70	7.10	13.43	-0.386	-0.733	
8	15.0	1.0	2.00	4.68	9.10	5.01	9.95	-0.336	-0.846	
9	67.5	5.5	0.50	10.04	13.71	8.99	14.63	1.050	-0.919	
10	67.5	5.5	1.25	9.39	15.19	9.38	14.64	0.013	0.543	
11	15.0	10.0	0.50	6.16	13.73	6.93	13.90	-0.772	-0.172	*1
12	67.5	5.5	1.25	9.39	15.19	9.38	14.64	0.013	0.543	
13	120.0	1.0	2.00	6.33	14.15	5.55	13.57	0.782	0.579	
14	120.0	10.0	2.00	4.02	9.14	3.77	9.31	0.248	-0.164	*3
15	67.5	10.0	1.25	5.78	9.72	6.00	11.78	-0.218	-2.060	
16	67.5	5.5	1.25	9.39	15.19	9.38	14.64	0.013	0.543	
17	67.5	5.5	2.00	6.99	11.70	8.08	12.41	-1.090	-0.709	
18	15.0	1.0	0.50	5.76	13.04	6.00	12.47	-0.238	0.571	
19	15.0	5.5	1.25	11.11	14.00	10.16	14.69	0.951	-0.693	*2
20	120.0	10.0	0.50	4.96	12.47	4.61	11.22	0.346	1.250	

Note: RAW sample actual values for MOE and MCF are 3.16 MPa and 11.51 KN, respectively.
*1 Highlighted is nearest optimal conditions of actual and predicted values.
*2 Highlighted is the highest actual and predicted values.
*3 Highlighted is the lowest actual and predicted values.

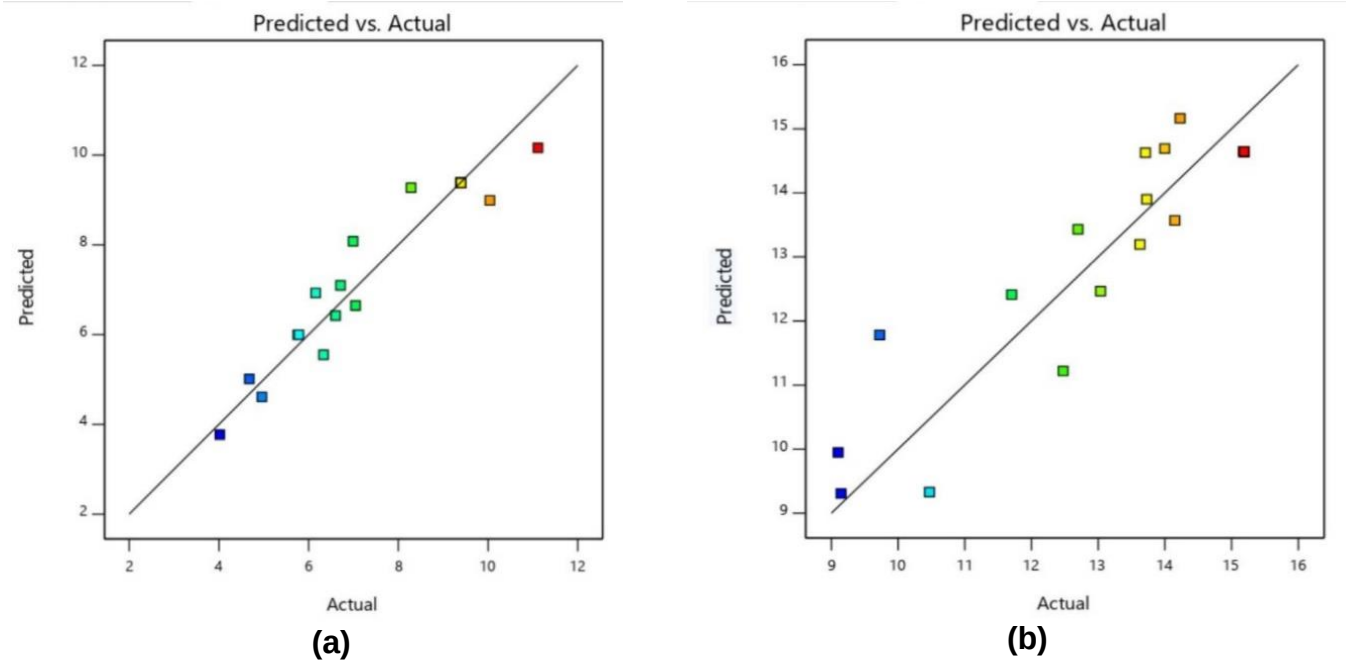

(a) (b)

Fig. 2. The model plots of the predicted and actual values for (a) MOE, and (b) MCF

Prediction of Optimal Conditions

The most significant feature of this research was to improve the mechanical characteristics of the impregnated organoclay/PMFM pulai wood samples. The MOE and MCF were optimized by minimizing the quantity of PMFM, organoclay, and the effect of time. The surface plot for optimization of MOE is shown in Fig. 3. The optimal value of MOE was 9.23 MPa, with 15 min, 4.19 wt% of PMFM, and 0.5 wt% of organoclay. Equally, the optimum value of the MCF at the same conditions was 14.95 kN. This can be seen in Fig. 4. The optimum circumstances for producing impregnated organoclay/PMFM pulai wood samples are these optimized values. Shorter or longer time may influence the result in deterioration of mechanical characteristic or a high cost due to chemical waste. Similarly, preparations that are short time of treatment may result in less effective treatment (Rahman *et al.* 2021).

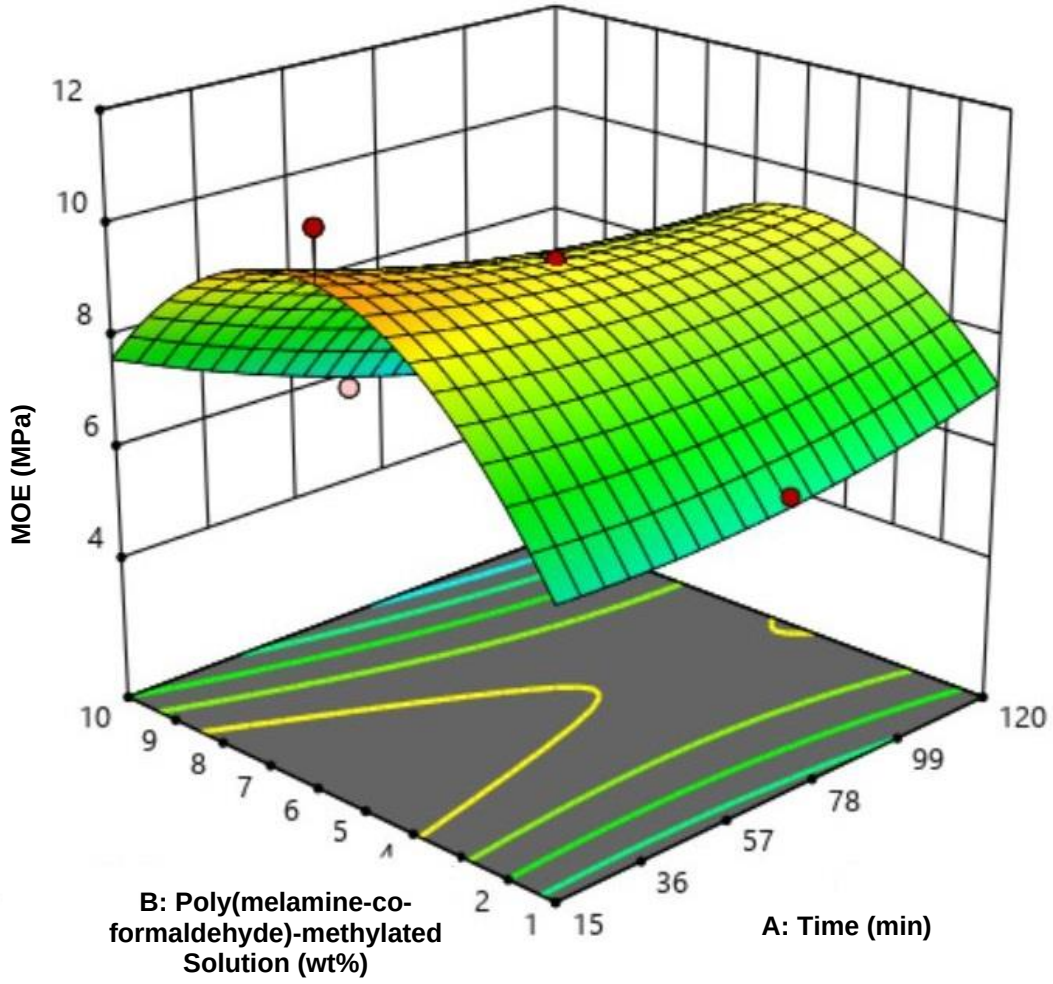

Fig. 3. Surface plot for optimization of MOE

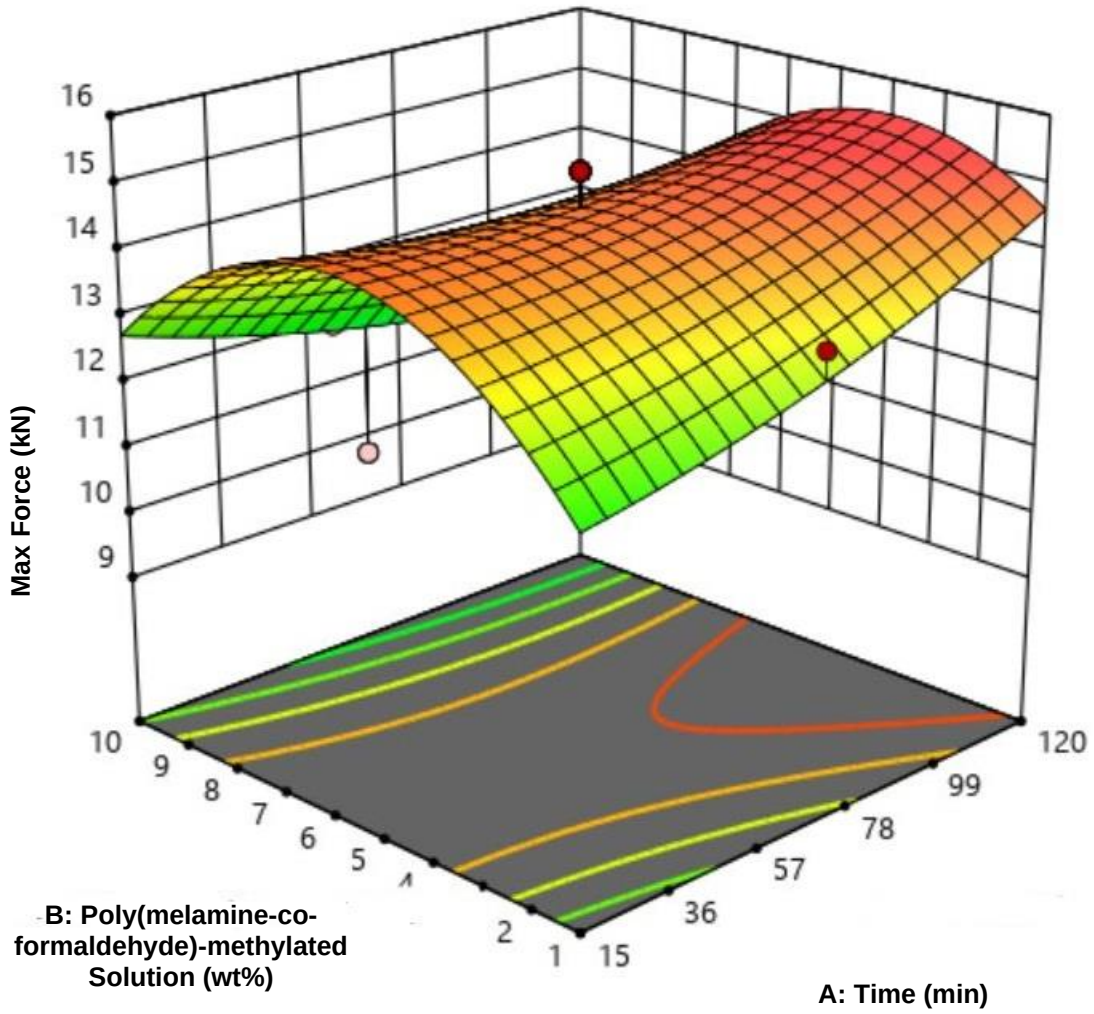

Fig. 4. Surface plot for optimization of MCF

Mechanical Properties

The compression test was conducted to analyze the MOE and MCF properties. The average values of MOE and MCF are reported in Table 6. From Table 6 (after considering the optimal conditions values obtained for MOE and MCF), the nearest optimum actual sample was Sample A2 with 15 min, 10.0 wt% of PMFM, and 0.5% of organoclay with MOE and MCF values of 6.16 MPa and 13.73 kN, respectively. However, without considering the optimum conditions, the highest MOE and MCF for actual sample was Sample B5 with 15 min, 5.5 wt% of PMFM, and 1.25% of organoclay with MOE and MCF values of 11.11 MPa and 14.00 kN, respectively. Meanwhile, without considering the optimum conditions, the lowest MOE and MCF for actual sample was Sample C1 with 120 min, 10.0 wt% of PMFM, and 2.00% of organoclay with MOE and MOF values of 4.02 MPa and 9.14 kN, respectively. It is noted that duration, composition ratio of PMFM, and organoclay used highly influenced the properties of the samples. Longer duration of impregnation deteriorated the sample, less PMFM, or less organoclay did not improve the sample properties, which was also confirmed by many other researchers (Adamu *et al*. 2020, 2021; Jiang *et al*. 2020; Rahman *et al*. 2021).

Infrared Spectral Properties

Infrared spectra for raw and impregnated organoclay/PMFM *pulai* wood samples were recorded in the infrared wavelength range of 4000 to 400 cm^{-1}, as shown in Figs. 5 through 8. During the chemical treatment, chemical breakdown and duration fluctuate, resulting in varying peak values. A similar curve for the treated impregnated organoclay/PMFM pulai wood samples revealed the presence of hemicelluloses, cellulose, and lignin. The OH stretching groups on the cellulose molecules and CH stretching vibrations caused the wide peaks between 3600 to 3000 cm^{-1}, and 3000 to 2800 cm^{-1}, respectively (Báder *et al*. 2020). The acetyl and ester groups of hemicellulose, or the ester linkage of carboxylic groups of ferulic and *p*-coumaric acids of lignin or hemicellulose, were ascribed to the significant peak intensities of the impregnated organoclay/PMFM pulai wood samples in the area between 1800 and 1700 cm^{-1}. The absorbed water was in the range of 1700 to 1600 cm^{-1} for both raw and impregnated organoclay/PMFM pulai wood samples (Ivashchenko *et al*. 2016). The CH_2 bending vibrations caused the peak area between 1600 and 1200 cm^{-1}. The peak intensities of the impregnated organoclay/PMFM pulai wood samples decreased across the wavenumber when lignin was partially removed (Oushabi *et al.* 2017). Increases in cellulose content can be seen in the peak intensities between 1200 to 400 cm^{-1}, which was due to polymerization with organoclay and PMFM (Jayamani *et al*. 2020; Zhang *et al.* 2020). The impregnated organoclay/PMFM pulai wood samples experienced a chemical impregnation alteration, which changed the compositional and mechanical characteristics of the sample, according to the FTIR data provided.

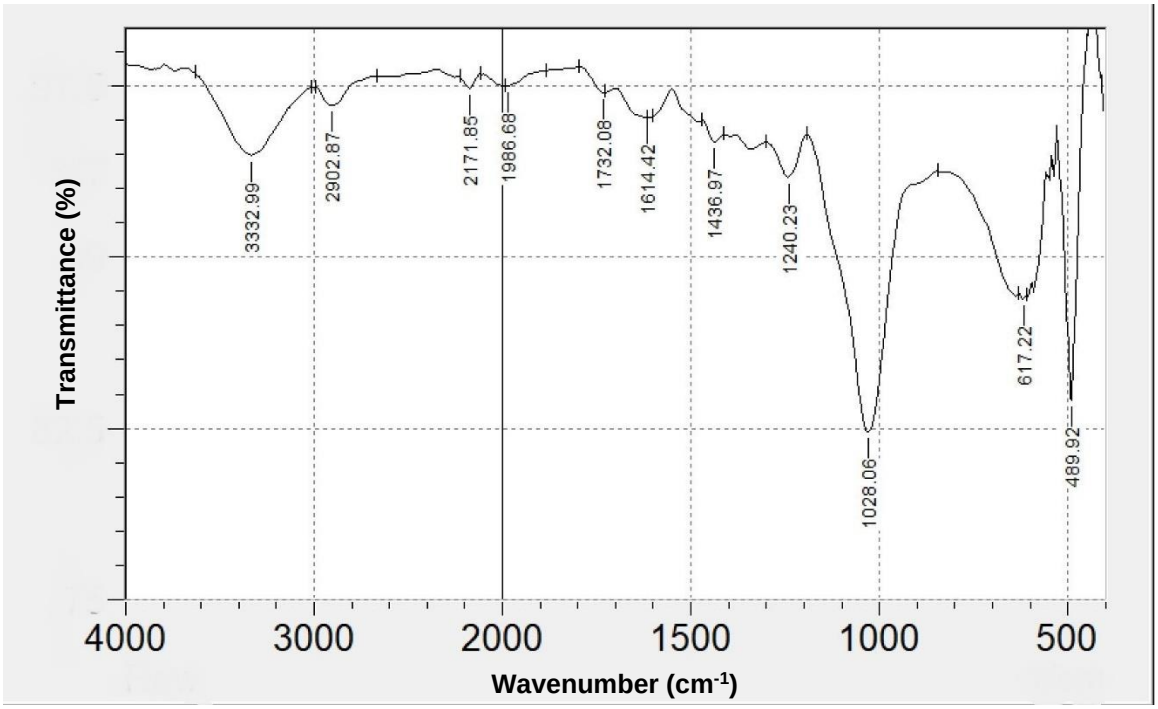

Fig. 5. FTIR results of raw pulai wood sample

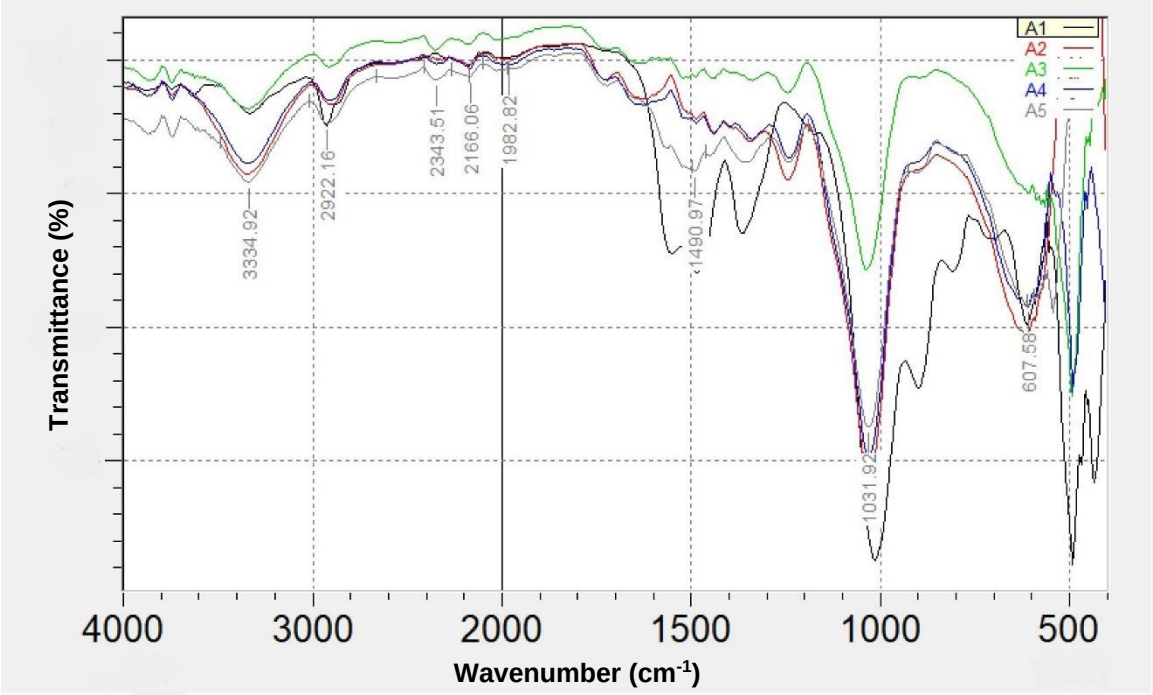

Fig. 6. FTIR results for impregnated organoclay/poly(melamine-co-formaldehyde)-methylated pulai wood samples of A1, A2, A3, A4, and A5 samples

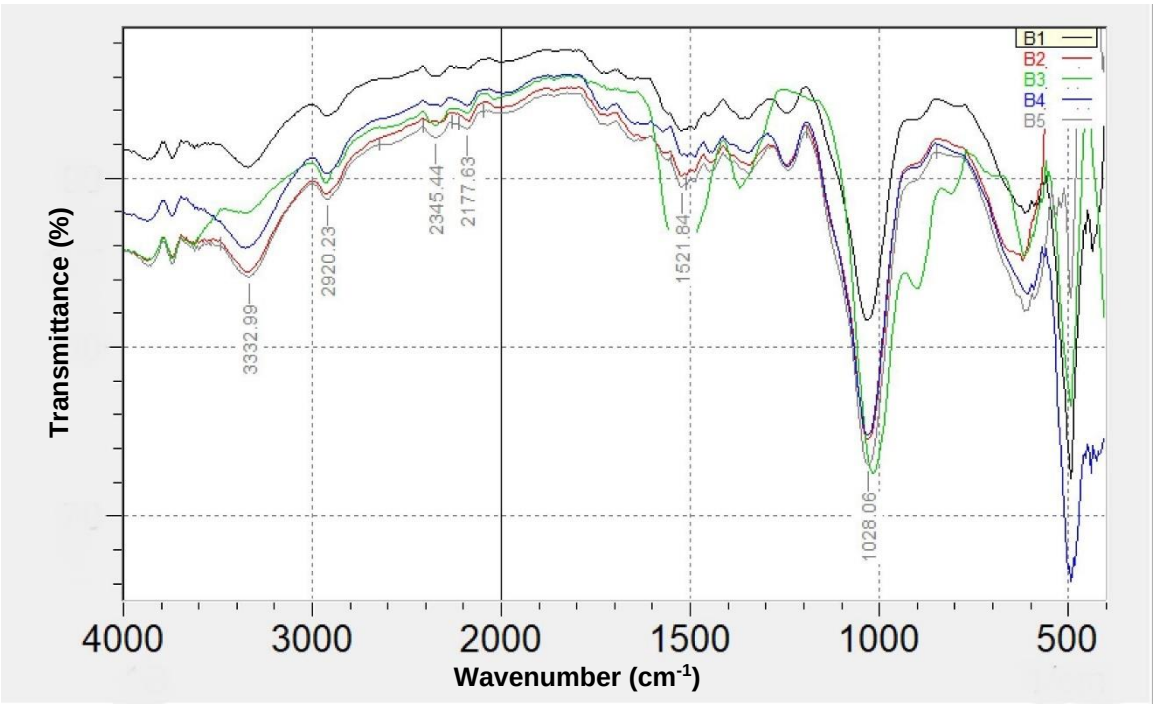

Fig. 7. FTIR results for impregnated organoclay/poly(melamine-co-formaldehyde)-methylated pulai wood samples of B1, B2, B3, B4, and B5 samples

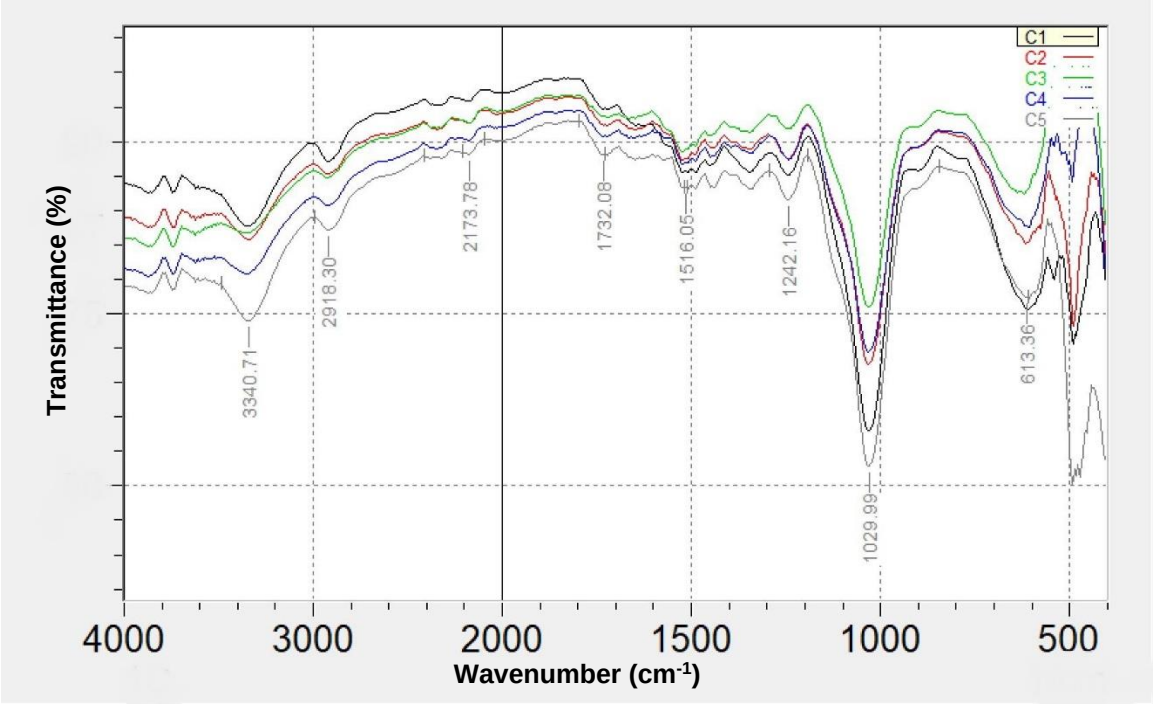

Fig. 8. FTIR results for impregnated organoclay/poly(melamine-co-formaldehyde)-methylated *pulai* wood samples of C1, C2, C3, C4, and C5 samples

Morphological Properties

The surface morphology of raw and impregnated organoclay/PMFM pulai wood samples are presented in Figs. 9 through 12. The raw pulai wood in Fig. 9 clearly displays hollow lumen structures of the wood fiber, especially on the surface. Figures 10, 11, and 12 indicate that the hollow lumen, pores, or void structures were filled with organoclay, and the surface structure of all samples was altered by the PMFM. The outside surface of the cell lumens also interacted with the organoclay/PMFM due to homogeneous polymerization (Devi and Maji 2012; Zhang *et al.* 2020). Because the hydroxyl group of the impregnated organoclay/PMFM pulai wood sample reacted with organoclay and PMFM, impregnated organoclay/PMFM was formed. Organoclay and PMFM polymerization, as well as dispersion of organoclay and PMFM into hollow lumen structures, pores, or voids, generated the morphology (Devi and Maji 2012; Zhang *et al.* 2020). Materials with strong interface adhesion and strengthened cohesive bonds were formed because of the copolymerization, which improved mechanical strength and thermal stability (Adamu *et al.* 2020, 2021). The chemical composition of the organoclay/PMFM combination in samples A1 and A2 was similar, but the impregnation period was different. Sample A1 required 120 min to complete, whereas sample A2 took just 15 min to complete the chemical treatment procedure. As a result, the impregnation period had a significant impact on the shape of the produced samples. From here, the longer duration sample appeared to have deteriorated, causing the structure to be tightly packed with organoclay and PMFM mixture, resulting in lower MOE and MCF values (Broda *et al.* 2019).

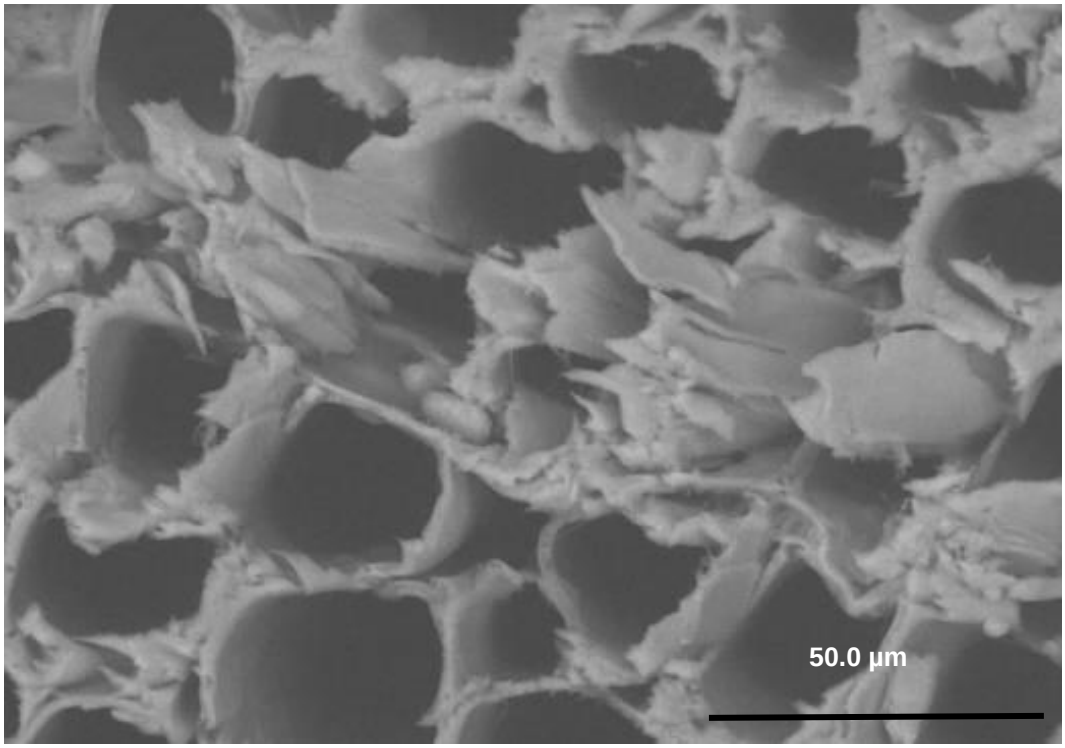

Fig. 9. SEM image of raw pulai wood sample

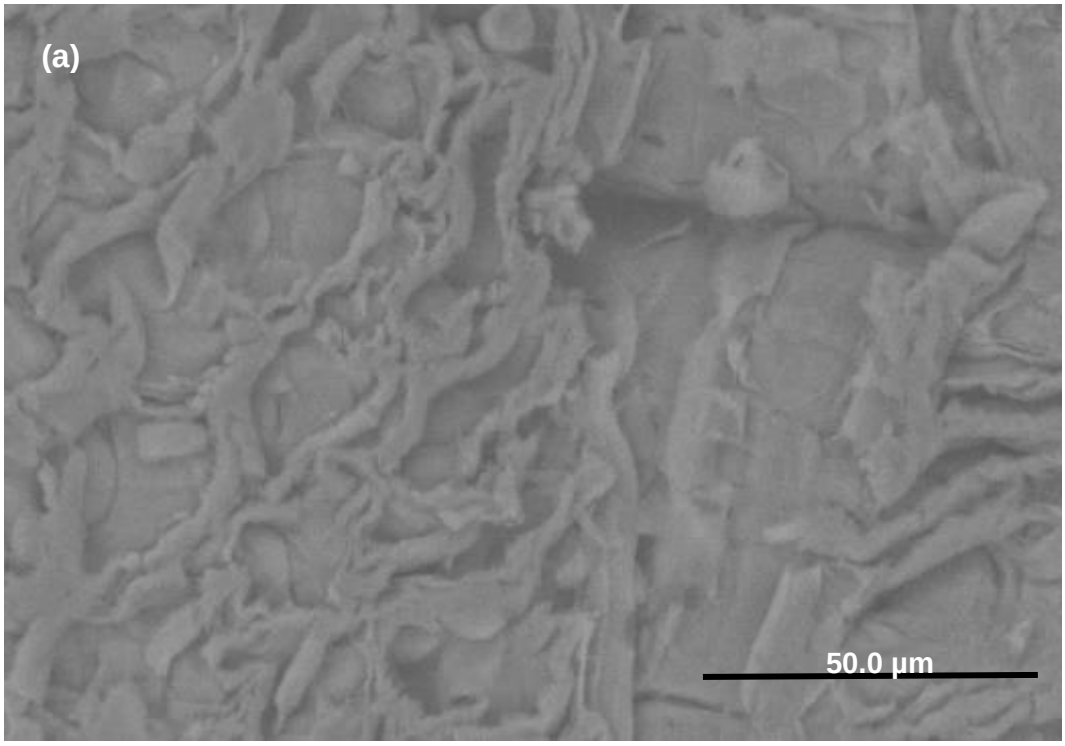

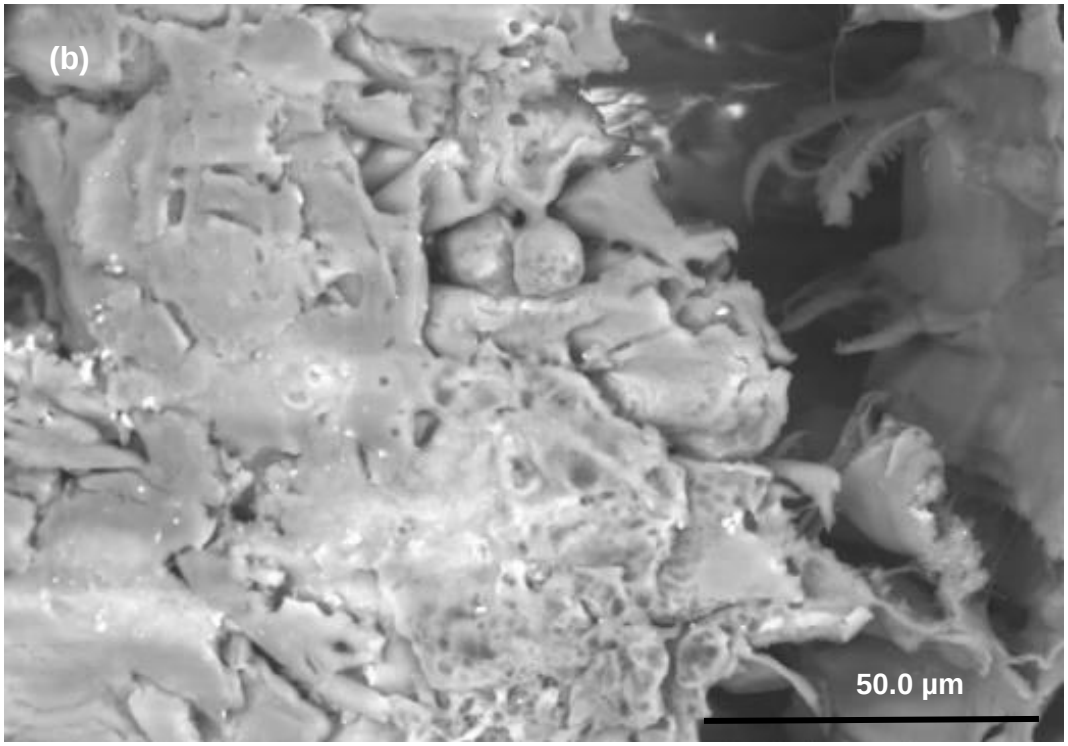
(b)
50.0 µm

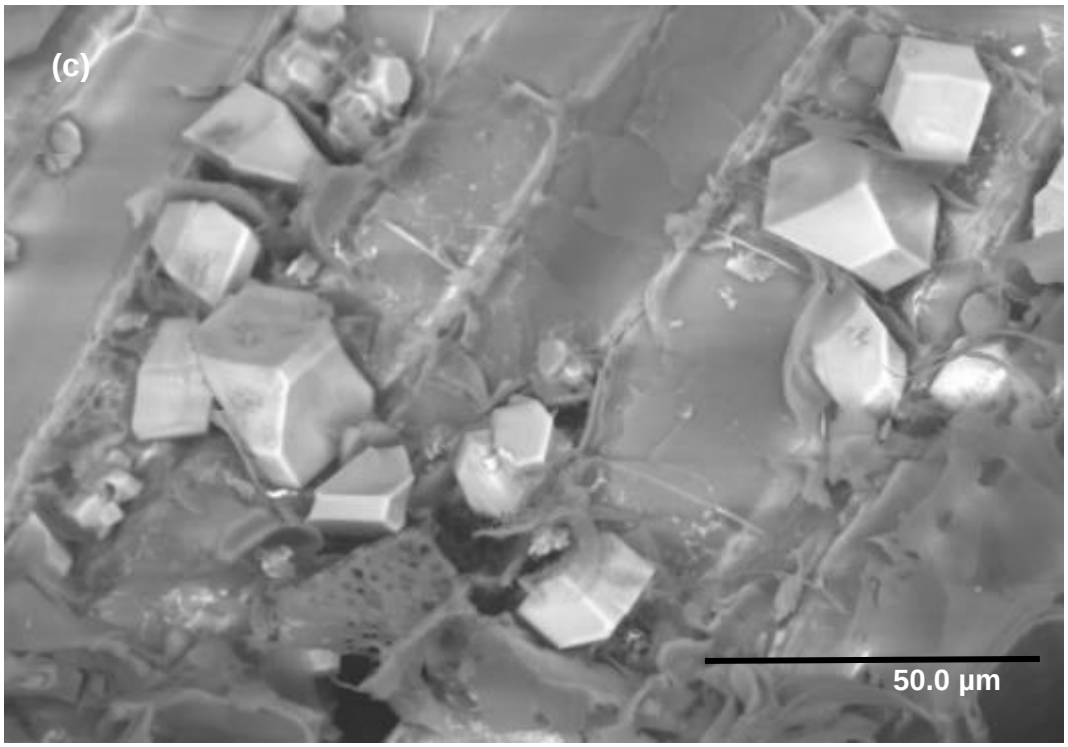
(c)
50.0 µm

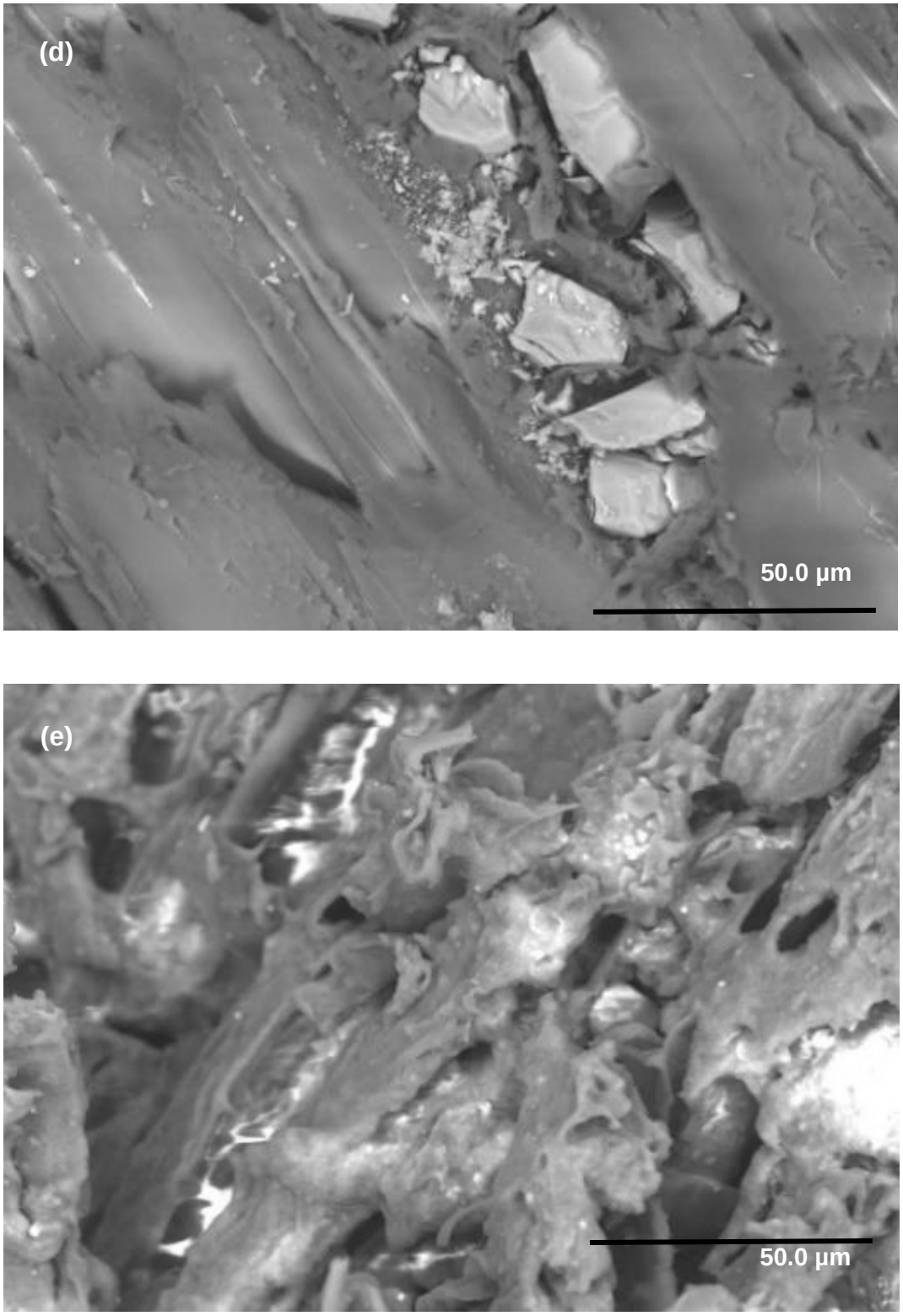

Fig. 10. SEM images for impregnated organoclay/poly(melamine-co-formaldehyde)-methylated pulai wood samples of (a) A1, (b) A2, (c) A3, (d) A4, and (e) A5

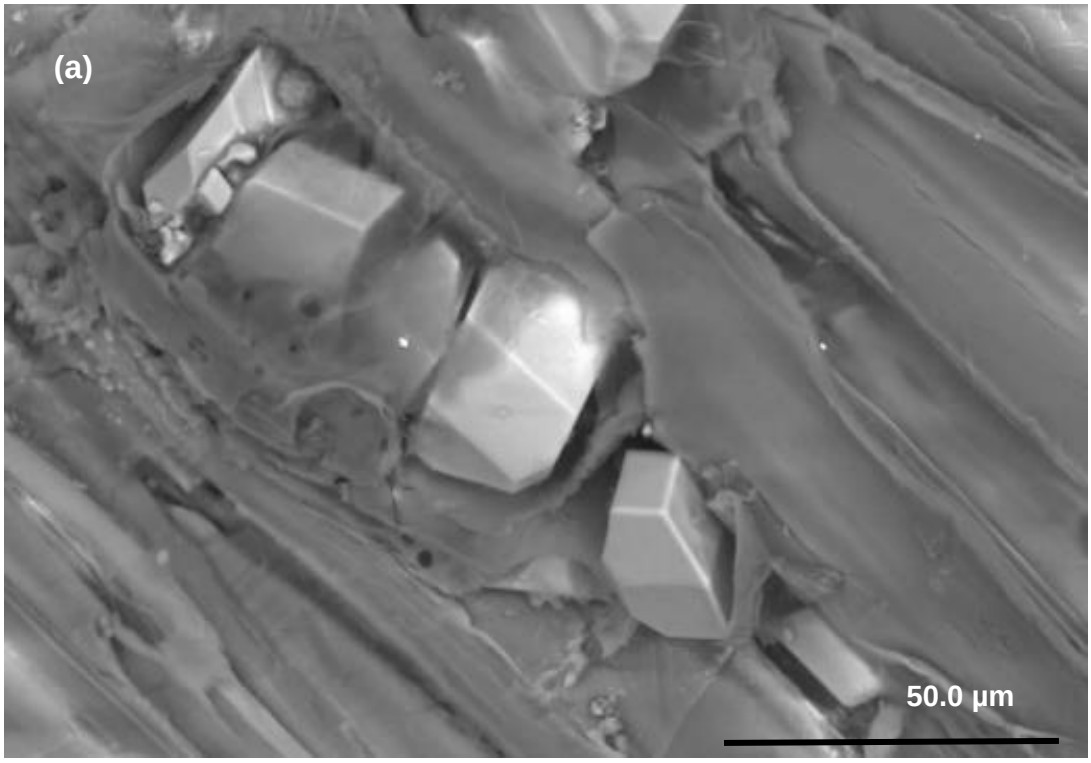
(a)
50.0 µm

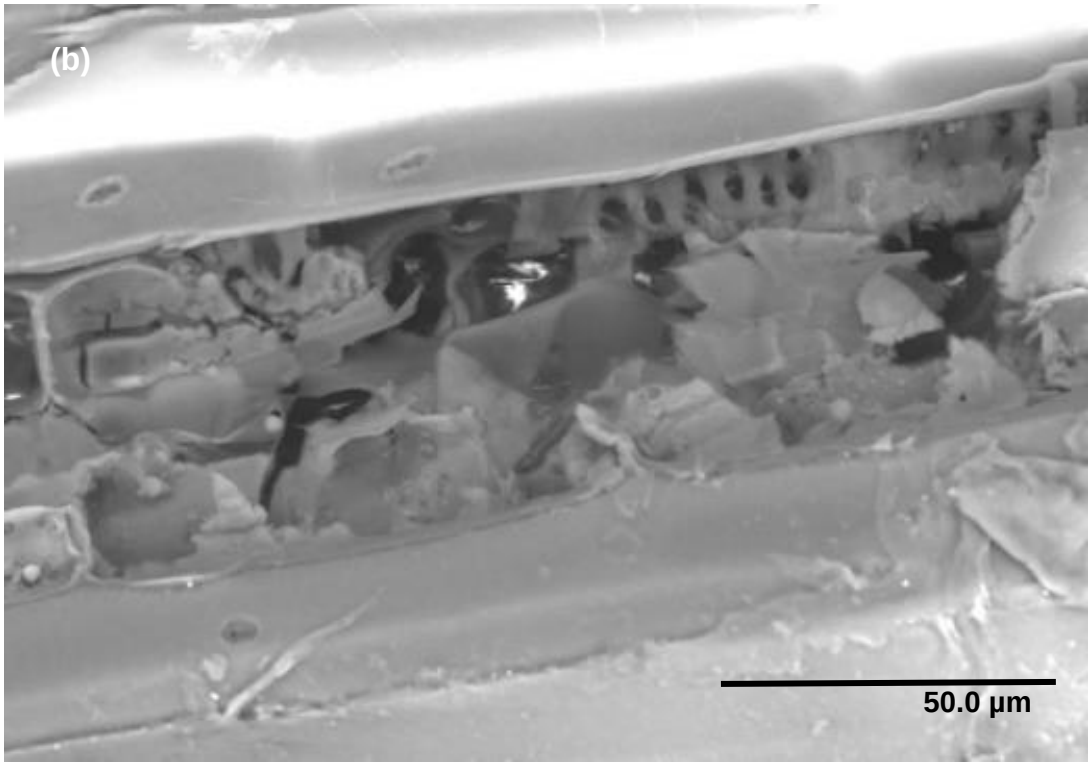
(b)
50.0 µm

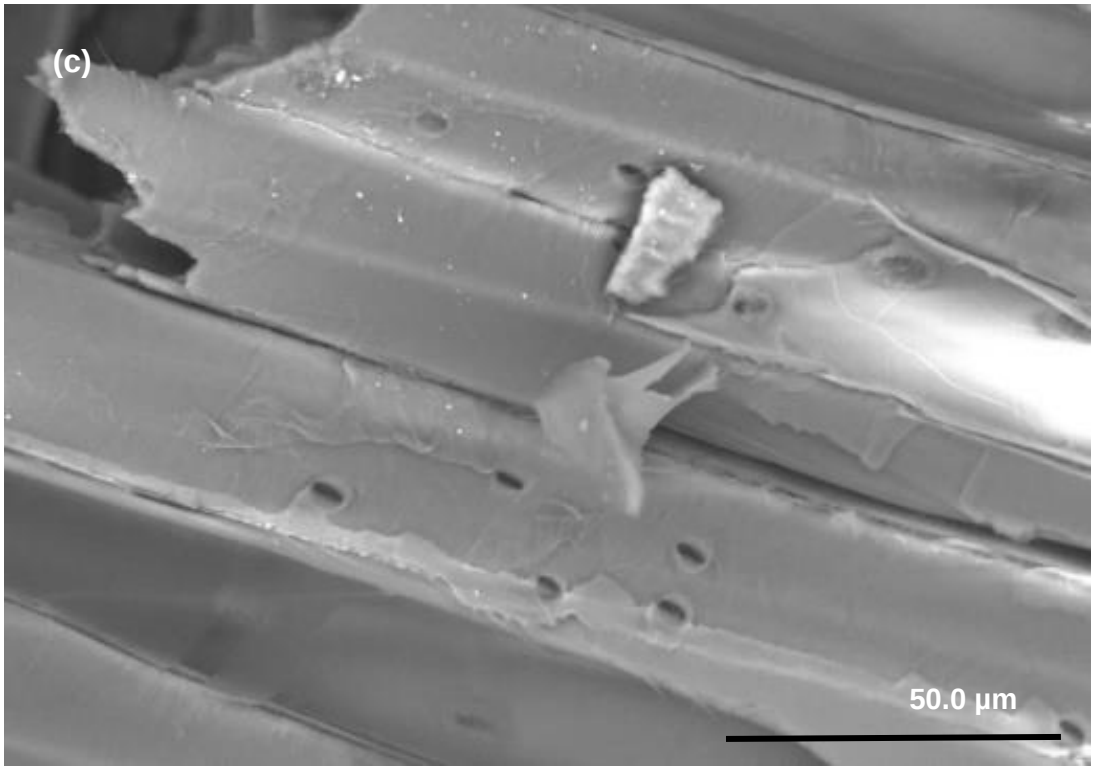
(c)
50.0 µm

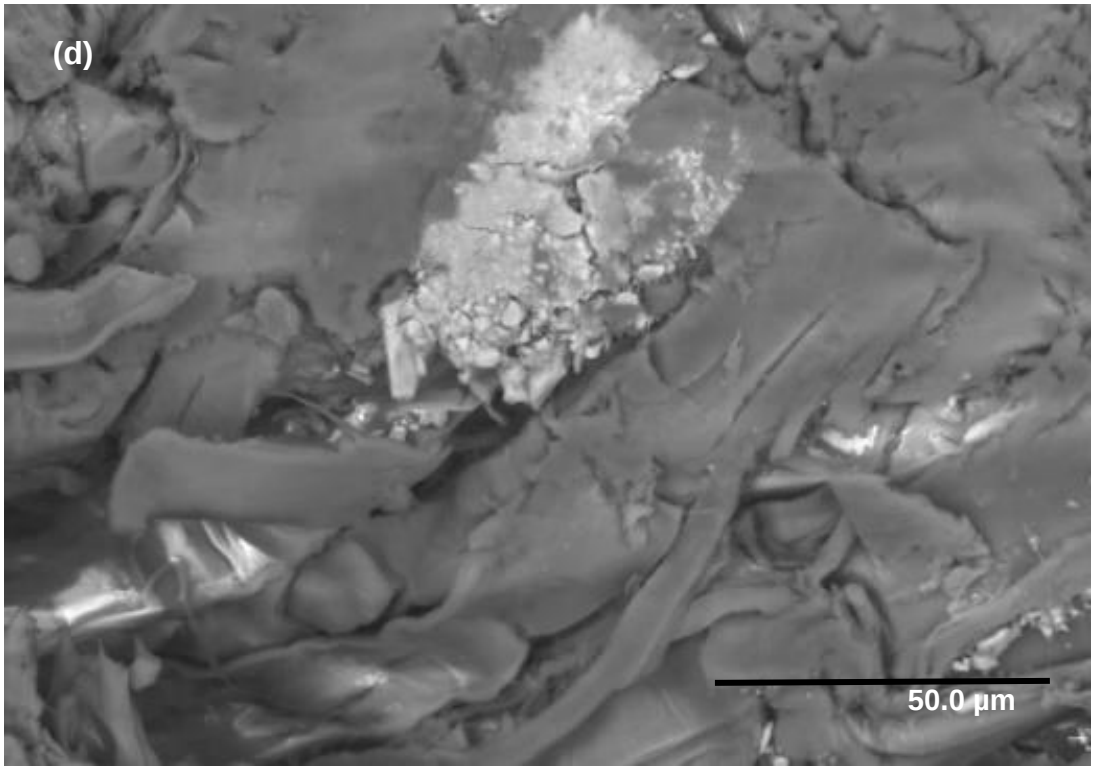
(d)
50.0 µm

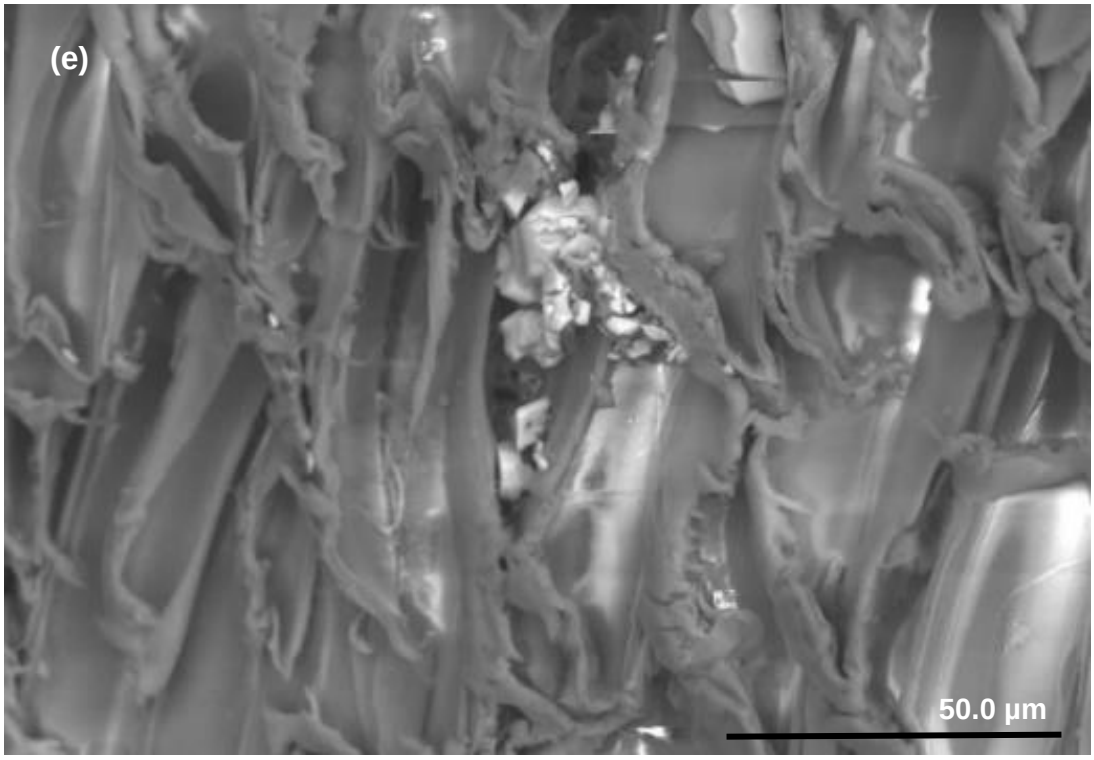

Fig. 11. SEM images for impregnated organoclay/poly(melamine-co-formaldehyde)-methylated *pulai* wood samples of (a) B1, (b) B2, (c) B3, (d) B4, and (e) B5

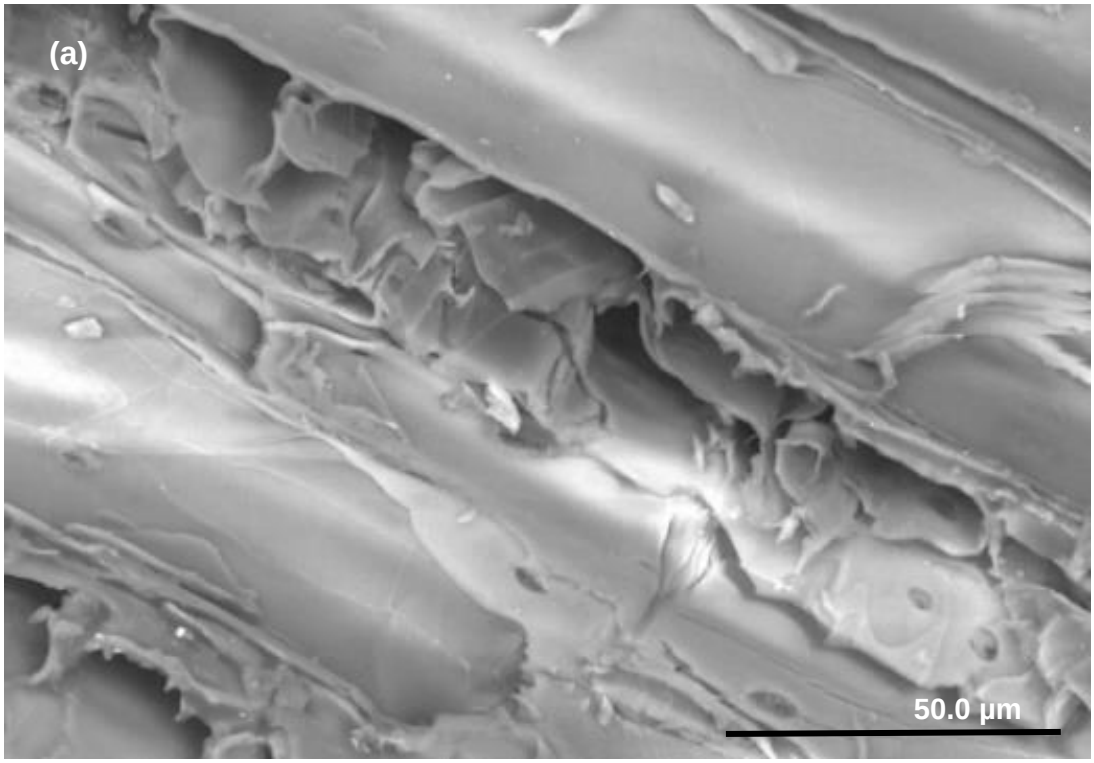

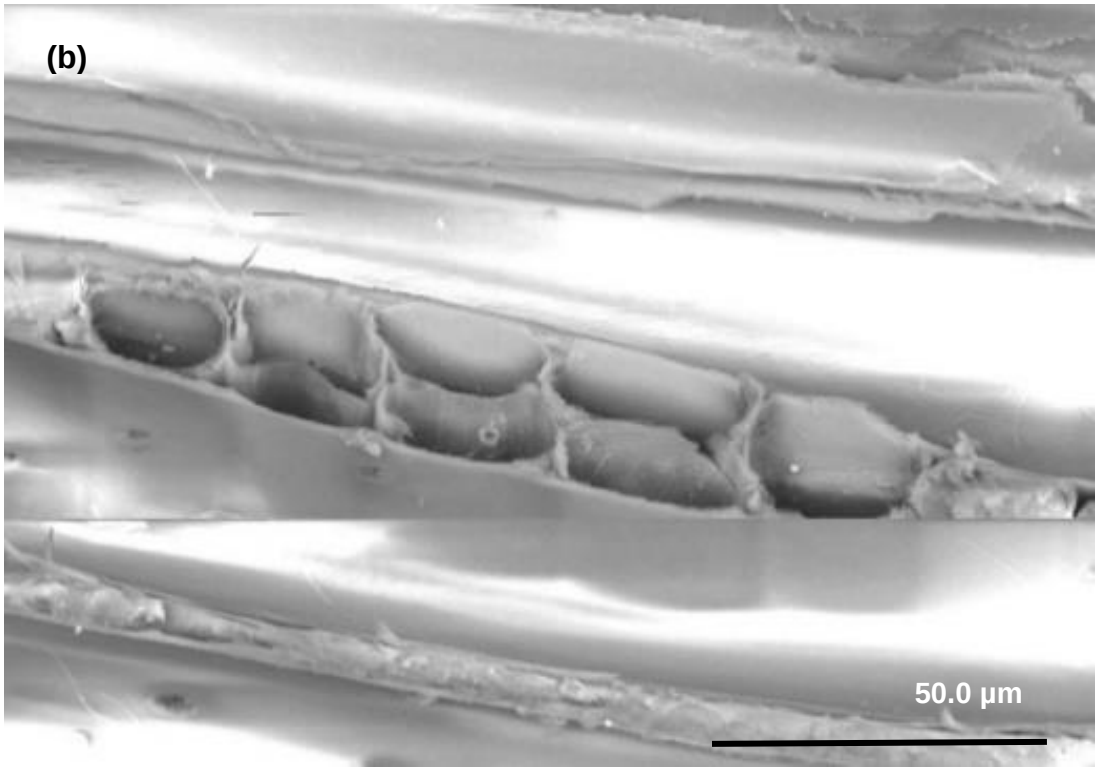
(b)
50.0 µm

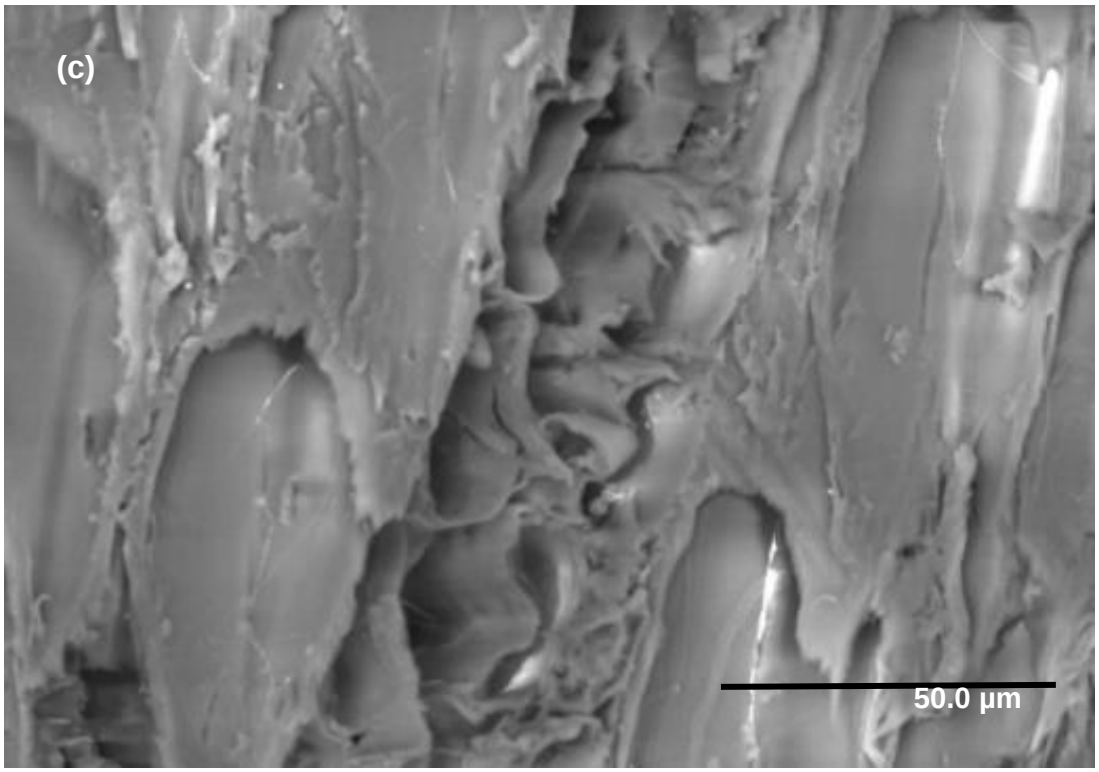
(c)
50.0 µm

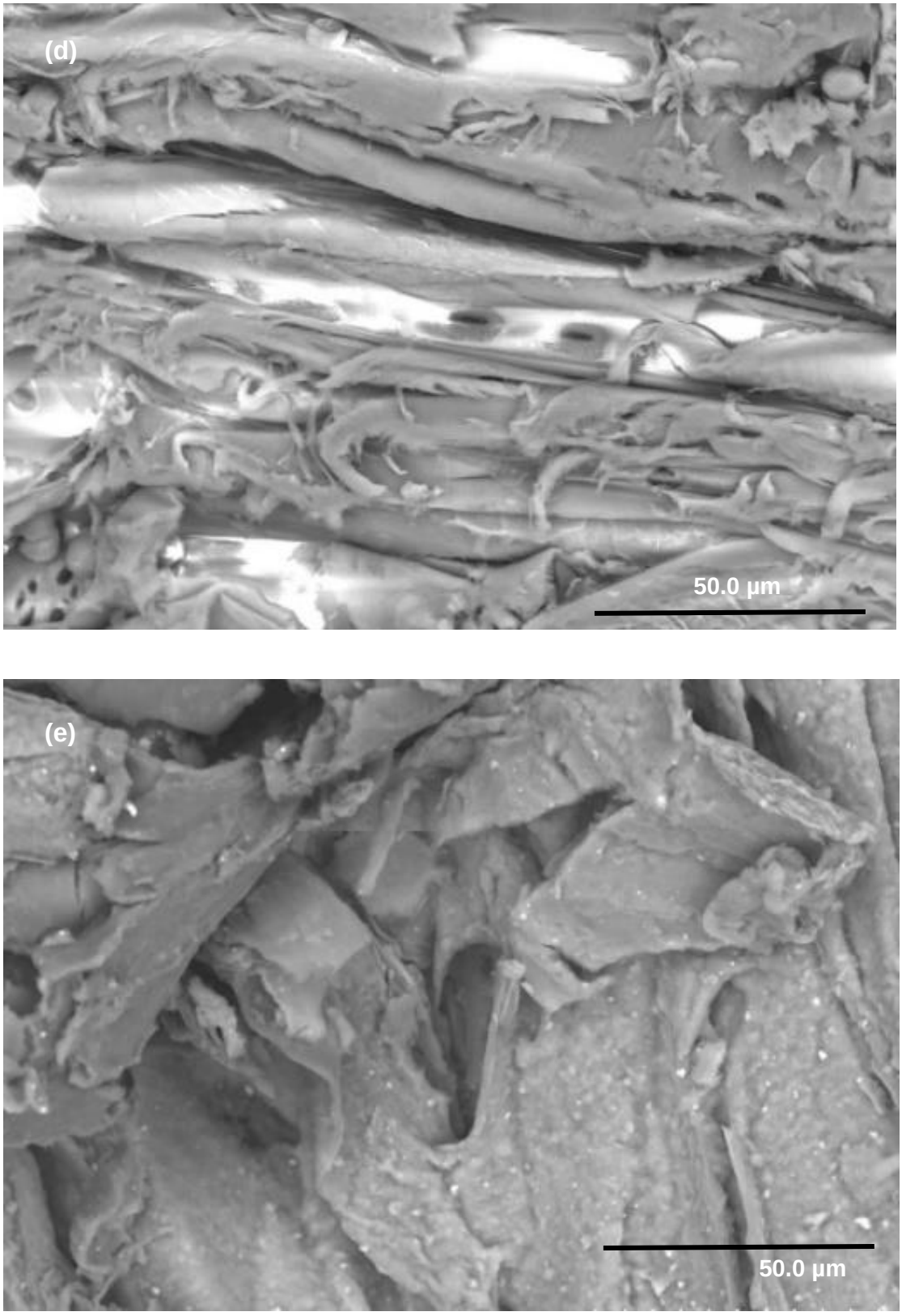

Fig. 12. SEM images for impregnated organoclay/poly(melamine-co-formaldehyde)-methylated pulai wood samples of (a) C1, (b) C2, (c) C3, (d) C4, and (e) C5

Elemental/Chemical Composition Properties

The elemental concentrations, based on EDS/EDX, for both raw and impregnated organoclay/PMFM pulai wood samples are presented in Tables 7 through Table 10. For all the samples, the primary elements found were carbon (C) and oxygen (O), confirming the basic features of wood elemental properties with the highest content for both mass and atom percentage (da Silva *et al*. 2019; Zhao *et al*. 2019). Nitrogen (N), silicon (Si), aluminum (Al), calcium (Ca), indium (In), antimony (Sb), ruthenium (Ru), sodium (Na), rubidium (Rb), iron (Fe), magnesium (Mg), and chlorine (Cl) were all present after impregnation of organoclay/PMFM into the samples. This indicated that during the impregnation of the organoclay/PMFM into the wood samples the structure and composition of the samples was altered. This would result in a potential chemical composition on the wood's surface with chemicals like NO_3, $CaCO_3$, Al_2O_3, MgO, SiO, SiO_2, and Na_2O

Table 7. EDS/EDX Elemental Result of Raw Pulai Wood Sample

Element	Raw	
	Mass (%)	Atom (%)
C	57.69	64.50
O	42.31	35.50
Sum	**100.00**	**100.00**

Table 8. EDS/EDX Elementals Result for Impregnated Organoclay/ Poly(Melamine-co-formaldehyde)-methylated Pulai Wood Samples of (a) A1, (b) A2, (c) A3, (d) A4, and (e) A5

Element	A1		A2		A3		A4		A5	
	Mass (%)	Atom (%)	Mass (%)	Atom (%)	Mass (%)	Atom (%)	Mass (%)	Atom (%)	Mass (%)	Atom (%)
C	58.18	64.95	48.67	55.34	56.46	63.49	55.74	63.05	44.74	51.30
O	41.82	35.05	38.37	32.75	43.07	36.35	43.13	36.63	36.45	31.37
N	-	-	11.42	11.14	-	-	-	-	16.43	16.15
Si	-	-	0.96	0.47	-	-	-	-	1.25	0.61
Al	-	-	0.58	0.29	-	-	-	-	1.13	0.57
Ca	-	-	-	-	0.47	0.16	0.86	0.29	-	-
In	-	-	-	-	-	-	0.28	0.03	-	-
Sum	**100.0**	**100.0**	**100.0**	**100.0**	**100.0**	**100.0**	**100.0**	**100.0**	**100.0**	**100.0**

Table 9. EDS/EDX Elementals Result for Impregnated Organoclay/ Poly(Melamine-co-formaldehyde)-methylated Pulai Wood Samples of (a) B1, (b) B2, (c) B3, (d) B4, and (e) B5

Element	B1		B2		B3		B4		B5	
	Mass (%)	Atom (%)	Mass (%)	Atom (%)	Mass (%)	Atom (%)	Mass (%)	Atom (%)	Mass (%)	Atom (%)
C	56.98	63.83	54.24	61.86	56.77	64.20	55.97	63.86	56.17	63.06
O	43.02	36.17	44.01	37.68	42.00	35.66	41.41	35.46	43.83	36.94
Ca	-	-	1.16	0.40	-	-	1.68	0.57	-	-
In	-	-	0.58	0.07	1.23	0.15	-	-	-	-
Sb	-	-	-	-	-	-	0.94	0.11	-	-
Sum	**100.0**	**100.0**	**100.0**	**100.0**	**100.0**	**100.0**	**100.0**	**100.0**	**100.0**	**100.0**

Table 10. EDS/EDX Elemental Results For Impregnated Organoclay/ Poly(Melamine-co-formaldehyde)-methylated Pulai Wood Samples of (a) C1, (b) C2, (c) C3, (d) C4, and (e) C5

Element	C1		C2		C3		C4		C5	
	Mass (%)	Atom (%)	Mass (%)	Atom (%)	Mass (%)	Atom (%)	Mass (%)	Atom (%)	Mass (%)	Atom (%)
C	57.43	64.24	62.42	68.87	55.93	63.29	57.50	64.31	60.85	47.58
O	42.57	35.76	47.59	31.13	42.45	36.07	42.50	45.69	54.50	31.93
N	-	-	-	-	-	-	-	-	19.61	13.15
Si	-	-	-	-	-	-	-	-	12.49	4.18
Al	-	-	-	-	0.49	0.25	-	-	5.85	2.04
Ru	-	-	-	-	0.58	0.078	-	-	-	-
Na	-	-	-	-	0.55	0.32	-	-	-	-
Rb	-	-	-	-	-	-	-	-	3.42	0.38
Fe	-	-	-	-	-	-	-	-	1.38	0.23
Mg	-	-	-	-	-	-	-	-	0.93	0.36
Cl	-	-	-	-	-	-	-	-	0.54	0.14
Sum	**100.0**	**100.0**	**100.0**	**100.0**	**100.0**	**100.0**	**100.0**	**100.0**	**100.0**	**100.0**

. Most of these present chemical compositions changed the structure, enabled polymerization, and protected the surface from degradation, whereas the presence of these chemical compositions serves to enhance the strength of the impregnated wood through bonding adhesion (da Silva *et al*. 2019; Zhao *et al*. 2019). While the ideal composition of these elements would improve the strength, if it is less or more than the optimal ratio, the samples may degrade and might lose the strength of the impregnated wood (da Silva *et al*. 2019; Zhao *et al*. 2019).

Thermal Properties

Differential scanning calorimetry

Differential scanning calorimetry curves of raw and impregnated organoclay/ PMFM pulai wood samples are shown in Figs. 13, 14, and 15. For raw pulai wood and impregnated organoclay/PMFM samples, the first endothermic peak was detected at 40 °C to 160 °C, indicating the evaporation of moisture or water from the samples. Chemical interaction and alteration, resulting in better interfacial adhesion between the wood cell wall, poly(melamine-co-formaldehyde)-methylated solution, and organoclay/PMFM samples, could explain the high tendency of impregnated organoclay/PMFM samples to replace, by interchange it with the moisture and water at a lower temperature, due to pressure during the impregnation (Guo *et al.* 2018). Around 160 to 220 °C, a second endothermic peak was found, indicating cellulose and hemicellulose breakdown. Exothermic combustion of lignin and hemicellulose occurs from 380 to 410°C for raw and impregnated organoclay/PMFM samples. Better interfacial bonding among the cell wall, organoclay, and organoclay/PMFM resulted in this combustion. The exothermic curve also indicated that continual heat transfer to the environment causes exothermic reaction and further hemicellulose and lignin breakdown (Ramiah 1970; Stevula *et al*. 2016). The heat flow of each specimen was influenced by the interfacial connection among the impregnated organoclay/PMFM samples fiber cells (Pielichowski and Pielichowska 2018).

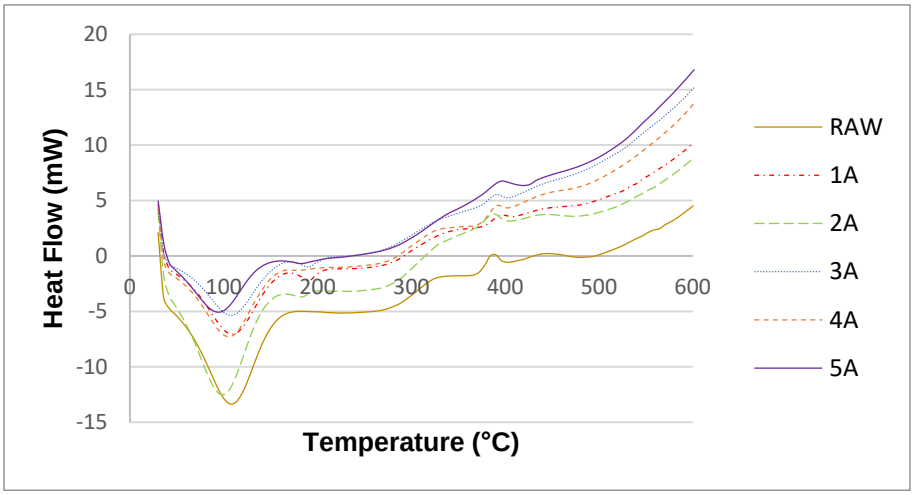

Fig. 13. DSC results for impregnated organoclay/poly(melamine-co-formaldehyde)-methylated pulai wood samples of (a) Raw, (b) A1, (c) A2, (d) A3, (e) A4, and (f) A5

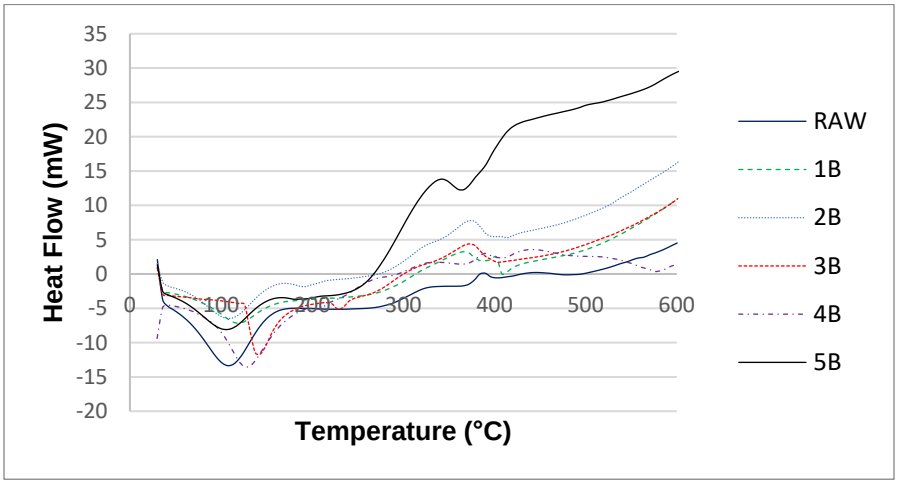

Fig. 14. DSC results for impregnated organoclay/poly(melamine-co-formaldehyde)-methylated pulai wood samples of (a) Raw, (b) B1, (c) B2, (d) B3, (e) B4, and (f) B5

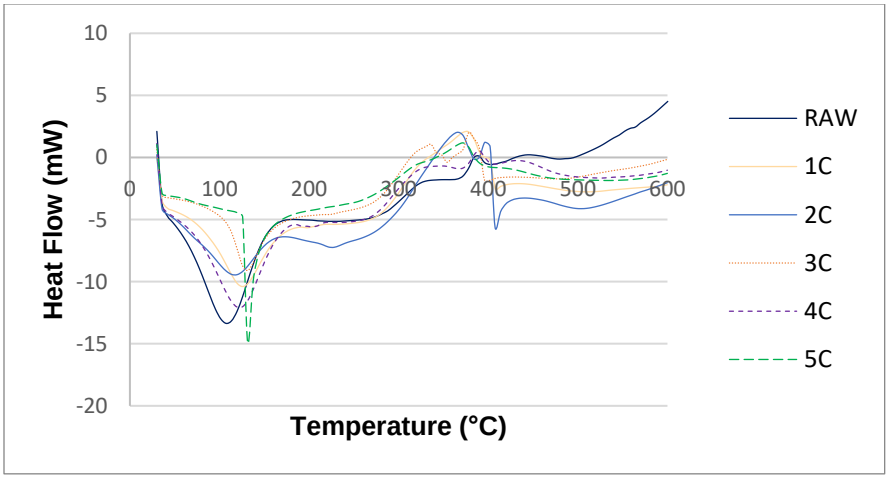

Fig. 15. DSC results for impregnated organoclay/poly(melamine-co-formaldehyde)-methylated pulai wood samples of (a) Raw, (b) C1, (c) C2, (d) C3, (e) C4, and (f) C5

Thermogravimetric analysis (TGA)

The thermograms of raw and impregnated organoclay/PMFM pulai wood samples are shown in Figs. 16, 17, and 18. The raw sample starting decomposition or onset temperature (T_o) is similar to other wood samples where breakdown occurs below 100 °C (Oushabi *et al.* 2017). In contrast, the initial decomposition temperature (T_i) and maximum decomposition temperature (T_m) of impregnated organoclay/PMFM samples were much greater than those of raw samples.

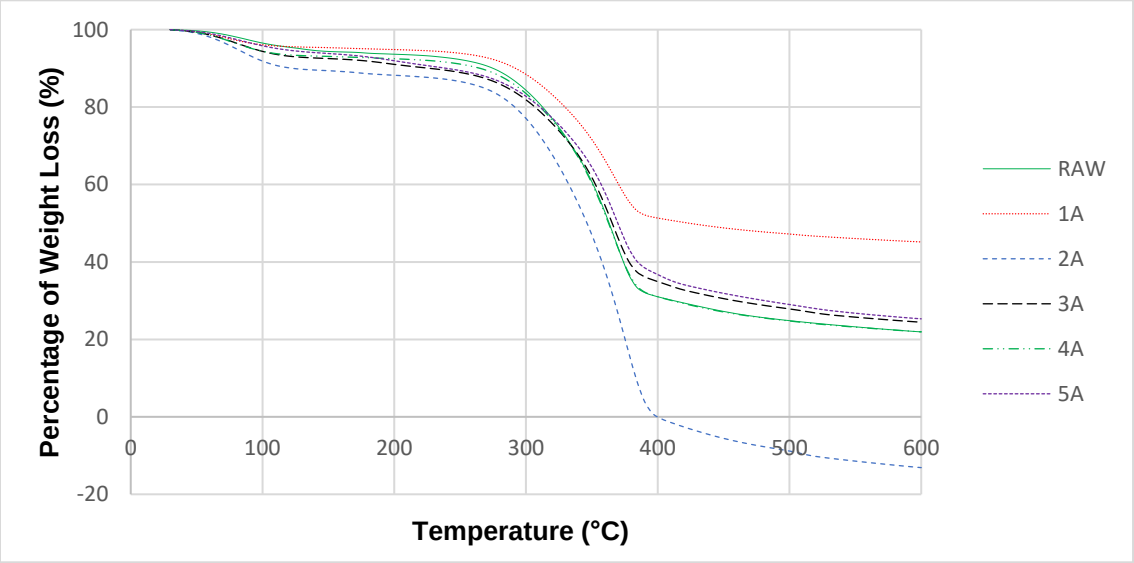

Fig. 16. TGA result for impregnated organoclay/poly(melamine-co-formaldehyde)-methylated pulai wood samples images of (a) Raw, (b) A1, (c) A2, (d) A3, (e) A4, and (f) A5

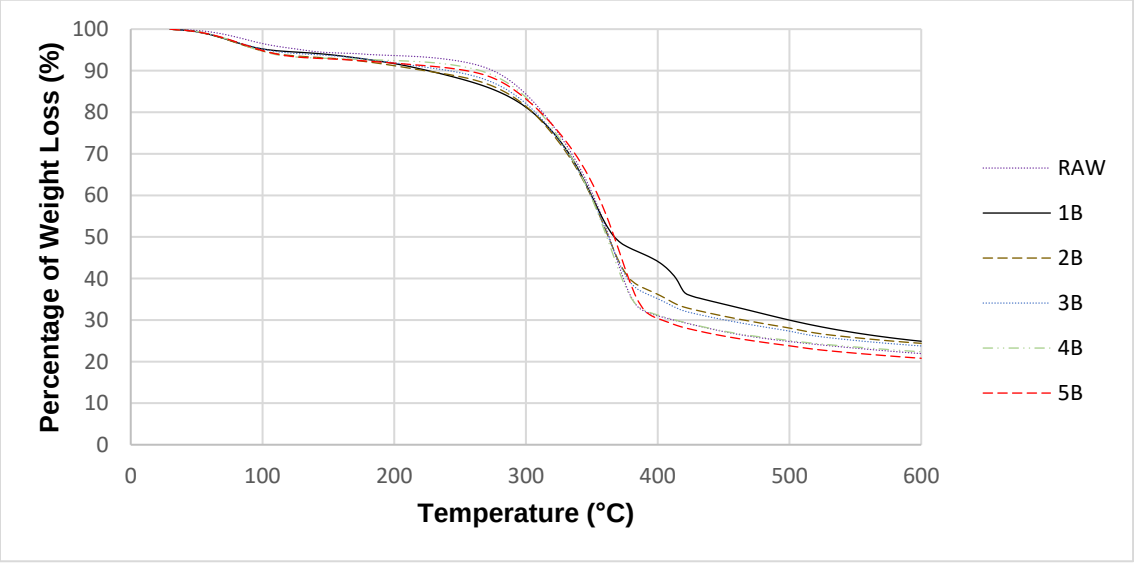

Fig. 17. TGA result for impregnated organoclay/poly(melamine-co-formaldehyde)-methylated pulai wood samples images of (a) Raw, (b) B1, (c) B2, (d) B3, (e) B4, and (f) B5

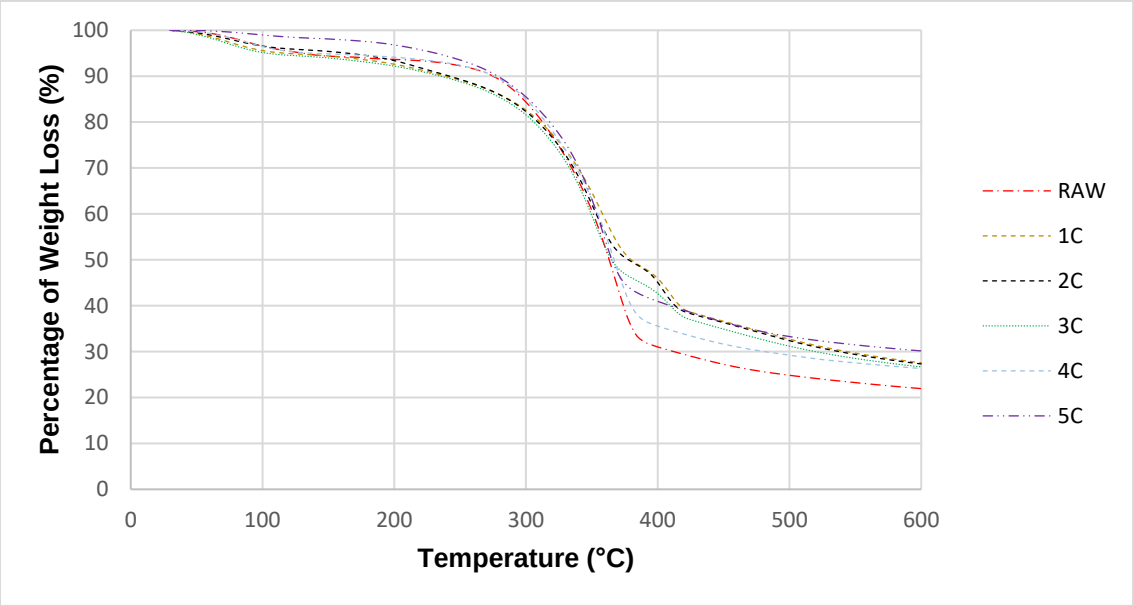

Fig. 18. TGA result for impregnated organoclay/poly(melamine-co-formaldehyde)-methylated pulai wood samples images of (a) Raw, (b) C1, (c) C2, (d) C3, (e) C4, and (f) C5

The results showed that samples impregnated with organoclay and PMFM were more thermally stable than raw samples. It is proposed that this was due to the high level of impregnation between the wood cell wall, organoclay, and PMFM. The integrated mixture of organoclay and PMFM was extensively polymerized and uniformly distributed across the samples and covered the surfaces, allowing for wood cell wall surface stabilization and barrier effects, which improved thermal stability. The mechanical characteristics of the impregnated organoclay/PMFM samples improved because of this. As a result, these methylated samples impregnated with organoclay/PMFM may be used to make construction and building materials. Clearly, this is a step forward, building upon other researchers' work (Adamu *et a*l. 2021). The FTIR and SEM analyses also yielded comparable results. On the pulai wood samples, all these findings support the copolymerization of impregnated organoclay and PMFM.

CONCLUSIONS

1. According to Design Expert 11 software, the highest modulus of elasticity (MOE) value was 9.23 MPa, 15 min, 4.19 wt% PMFM, and 0.5 wt% organoclay. Similarly, in the same circumstances, the MCF's optimal value was 14.95 kN. Sample A2 with 15 min, 10.0 wt% poly(melamine-co-formaldehyde)-methylated (PMFM), and 0.5 wt% of organoclay had MOE and maximum compression force (MCF) values of 6.16 MPa and 13.73 kN, respectively, for the closest real values.
2. The dispersion of the organoclay and polymerization of the organoclay and PMFM into the lumens of the pulai wood, as revealed by Fourier transform infrared (FTIR) results, indicated that there was dispersion of the organoclay and polymerization of the organoclay and PMFM into the lumens of the pulai wood.

3. The hydrophilicity of the impregnated organoclay/PMFM pulai wood samples decreased as the OH groups were reduced on the surface. In comparison to the raw sample, scanning electron microscopy (SEM) images of the impregnated organoclay/ PMFM samples revealed reduced void or pores spaces, strong interfacial bonding, smooth surfaces, and excellent dispersion of organoclay and PMFM samples revealed reduced void spaces and strong interfacial bond.
4. The differential scanning calorimetry (DSC) study revealed a low glass transition temperature. Those findings were supported by the thermogravimetric analysis (TGA) results, which revealed a low initial decomposition temperature for all samples. Organoclay and PMFM diffused on a nanoscale in the polymer matrix and worked as reinforcing fillers, resulting in enhanced mechanical characteristics and thermal stability, according to the characterization. As a result, the impregnated organoclay/PMFM samples generated may be employed in constructions and building materials.

ACKNOWLEDGMENTS

The authors would like to thank the 'Kementerian Pengajian Tinggi Malaysia, Fundamental Research Grant Scheme, RACER/1/2019/STG07/UNIMAS//1' for their financial support.

REFERENCES CITED

Adamu, M., Rahman, M. R., Bakri, M. K. B., Yusof, F. A. B. M., and Khan, A. (2021). "Characterization and optimization of mechanical properties of bamboo/nanoclay/ polyvinyl alcohol/styrene nanocomposites using response surface methodology," *Journal of Vinyl and Additive Technology* 27(1), 147-160. DOI: 10.1002/vnl.21792

Adamu, M., Rahman, M. R., Hamdan, S., Bakri, M. K. B., and Yusof, F. A. B. M. (2020). "Impact of polyvinyl alcohol/acrylonitrile on bamboo nanocomposite and optimization of mechanical performance by response surface methodology," *Construction and Building Materials* 258(1), article ID 119693. DOI: 10.1016/j.conbuildmat.2020.119693

ASTM D3418-15 (2015). "Standard test method for transition temperatures and enthalpies of fusion and crystallization of polymers by differential scanning calorimetry," ASTM International, West Conshohocken, PA, USA. DOI: 10.1520/D3418-15

ASTM D3501-05 (2018). "Standard test methods for wood-based structural panels in compression," ASTM International, West Conshohocken, PA, USA. DOI: 10.1520/D3501-05AR18

ASTM E1131-20 (2020). "Standard test method for compositional analysis by thermogravimetry," ASTM International, West Conshohocken, PA, USA. DOI: 10.1520/E1131-20

ASTM E1252-98 (2021). "Standard practice for general techniques for obtaining infrared spectra for qualitative analysis," ASTM International, West Conshohocken, PA, USA. DOI: 10.1520/E1252-98R21

ASTM E1269-11 (2018). "Standard test method for determining specific heat capacity by differential scanning calorimetry," ASTM International, West Conshohocken, PA, USA. DOI: 10.1520/E1269-11R18

ASTM E168-16 (2016). "Standard practices for general techniques of infrared quantitative analysis," ASTM International, West Conshohocken, PA, USA DOI: 10.1520/E0168-16

ASTM E2015-04 (2014). "Standard guide for preparation of plastics and polymeric specimens for microstructural examination," ASTM International, West Conshohocken, PA, USA. DOI: 10.1520/E2015-04R14

Báder, M., Németh, R., Sandak, J., and Sandak, A. (2020). "FTIR analysis of chemical changes in wood induced by steaming and longitudinal compression," *Cellulose* 28(1), 6811-6829. DOI: 10.1007/s10570-020-03131-8

Biziks, V., Bicke, S., and Militz, H. (2019). "Penetration depth of phenol-formaldehyde (PF) resin into beech wood studied by light microscopy," *Wood Science and Technology* 53(1), 165-176. DOI: 10.1007/s00226-018-1058-2

Bond, B. H., and Espinoza, O. (2016). "A decade of improved lumber drying technology," *Current Forestry Reports* 2(2), 106-118. DOI: 10.1007/s40725-016-0034-z

Broda, M., Curling, S. F., Spear, M. J., and Hill, C. A. S. (2019). "Effect of methyltrimethoxysilane impregnation on the cell wall porosity and water vapour sorption of archaeological waterlogged oak," *Wood Science and Technology* 53(20), 703-726. DOI: 10.1007/s00226-019-01095-y

da Silva, D. A., Eloy, E., Caron, B. O., and Trugilho, P. F. (2019). "Elemental chemical composition of forest biomass at different ages for energy purposes," *Floresta e Ambiente* 26(4), article ID e20160201. DOI: 10.1590/2179-8087.020116

De Meijer, M., and Militz, N. (1998). "Wet adhesion measurements of wood coatings," *Holz als Roh- und Werkstoff* 56, article no. 306. DOI: 10.1007/s001070050324

Devi, R. R., and Maji, T. K. (2012). "Effect of nano-SiO2 on properties of wood/polymer/clay nanocomposites," *Wood Science and Technology* 46(6), 1151-1168. DOI: 10.1007/s00226-012-0471-1

Foxworthy, F. W., and Woolley, H. W. (1930). "Durability of Malaysian timbers," *Malaysia Forest Record* 8(1), 37-43.

Guo, Y., Zhang, M., Xiao, Z., Chen, H., and Xie, Y. (2018). "Vaporization heat of bound water in wood chemically modified via grafting and crosslinking patterns by DSC and NMR analysis," *Holzforschung* 71(12), 1043-1049. DOI: 10.1515/hf-2017-0210

H'ng, P. S., Paridah, M. T., and Chin, K. L. (2010). "Bending properties of laminated veener lumber produced from Keruing (*Dipterocarpus* sp.) reinforced with low density wood species," *Asian Journal of Scientific Research* 3(2), 118-125. DOI: 10.3923/ajsr.2010.118.125

Homan, W. J., and Jorissen A. J. M. (2004). "Wood modification developments," *Heron* 49(4), 361-386.

How, S. S., and Nordahlia, A. S. (2018). "Delamination and adhesion strength of selected Malaysian timber for glue lamination: Pulai (*Alstonia* spp.)," *Timber Technology Bulletin* 2018, Article Number 85.

How, S. S., and Sik, H. S. (2020). "Adhesive bond performance of four Malaysian timber species in glue line delamination," *International Journal of Agriculture, Forestry and Plantation* 10(Sept), 125-132.

Ivashchenko, O., Jurga-Stopa, J., Coy, E., Peplinska, B., Pietralik, Z., and Jurga, S. (2016). "Fourier transform infrared and Raman spectroscopy studies on magnetite/Ag/antibiotic nanocomposites," *Applied Surface Science* 364(1), 400-409. DOI: 10.1016/j.apsusc.2015.12.149

Jayamani, E., Loong, T. G., and Bakri, M. K. B. (2020). "Comparative study of Fourier transform infrared spectroscopy (FTIR) analysis of natural fibres treated with chemical, physical and biological methods," *Polymer Bulletin* 77(1), 1605-1629. DOI: 10.1007/s00289-019-02824-w

Jiang, J., Chen, Y., Cao, J., and Mei, C. (2020). "Improved hydrophobicity and dimensional stability of wood treated with paraffin/acrylate compound emulsion through response surface methodology optimization," *Polymers* 12(1), Article Number 86. DOI: 10.3390/polym12010086

Kamke, F. A., and Lee, J. N. (2007). "Adhesive penetration in wood – A review," *Wood and Fiber Science* 39(2), 205-220.

Mader, A., Schirò, A., Brischetto, M., and Pizzo, B. (2011). "Interactions and penetration of polymers and nanolatexes into wood: An overview," *Progress in Organic Coatings* 71(2), 123-135. DOI: 10.1016/j.porgcoat.2011.02.007

Malaysian Timber Corporation (1982). "Pulai," (http://mtc.com.my/wizards/mtc_tud/items/report(91).php), Accessed 10 Nov 2021.

Mery, F., Ekamawanti, H. A., and Astiani, D. (2019). "Respons pertumbuhan bibit pulai (*Alstonia scholaris*) terhadap cuka kayu dan naungan [Growth response of island seedlings (*Alstonia scholaris*) to wood vinegar and shade]," *Jurnal Hutan Lestari* 7(3), 1321-1327. DOI: 10.26418/jhl.v7i3.37504

Monachino, J. (1949). "A revision of the genus *Alstonia* (*Apocynaceae*)," *Pacific Science* 3(2), 133-182.

Oktavia, R., Misfadhila, S., and Rivai, H. (2020). "Overview of traditional, phytochemical, and pharmacological uses of pulai (*Alstonia Scholaris*)," *World Journal of Pharmacy and Pharmaceutical Sciences* 9(8), 334-354. DOI: 10.20959/wjpps20208-16892

Oushabi, A., Sair, S., Hassani, F. O., Abboud, Y., Tanane, O., and El Bouari, A. (2017). "The effect of alkali treatment on mechanical, morphological, and thermal properties of date palm fibers (DPFs): Study of the interface of DPF–Polyurethane composite," *South African Journal of Chemical Engineering* 23(1), 116-123. DOI: 10.1016/j.sajce.2017.04.005

Pielichowski, K., and Pielichowska, K. (2018). "Polymer nanocomposites," in: *Handbook of Thermal Analysis and Calorimetry* (2nd Ed.), S. Vyazovkin, N. Koga, and C. Schick (eds.), Elsevier, Amsterdam, Netherlands, pp. 431-485. DOI: 10.1016/B978-0-444-64062-8.00003-6

Rahman, M. R., Muhammad, A., Hamdan, S., Bakri, M. K. B., Yusof, F. A. M., and Khan, A. (2021). "Optimization and characterization of acrylonitrile/MAPE/nano-clay bamboo nanocomposites by response surface methodology," *Polymer Bulletin* (Online), 1-29. DOI: 10.1007/s00289-021-03628-7

Ramiah, M. V. (1970). "Thermogravimetric and differential thermal analysis of cellulose, hemicellulose, and lignin," *Journal of Applied Polymer Science* 14(5), 1323-1337. DOI: 10.1002/app.1970.070140518

Stevula, N., Estokova, A., Cigasova, J., Schwarzova, I., Kacik, F., and Geffert, A. (2016). "Thermal degradation of natural and treated hemp hurds under air and nitrogen

atmosphere," *Journal of Thermal Analysis and Calorimetry* 128(1), 1659-1660. DOI: 10.1007/s10973-016-6044-z

Torgovnikov, G., and Vinden, P. (2009). "High-intensity microwave wood modification for increasing permeability," *Forest Products Journal* 59(4), 84-92.

Wong, T. M. (2002). *A Dictionary of Malaysia Timbers*, Forest Research Institute Malaysia, Kuala Lumpur, Malaysia.

Zhang, J., Liu, H., Yang, L., Han, T., and Yin Q. (2020). "Effect of moderate temperature thermal modification combined with wax impregnation on wood properties," *Applied Sciences* 10(22), article ID 8231. DOI: 10.3390/app10228231

Zhao, B., Yu, Z., Zhang, Y., and Qi, C. (2019). "Physical and mechanical properties of rubberwood (*Hevea brasiliensis*) dyed with *Lasiodiplodia theobromae*," *Journal of Wood Science* 65, article no. 63. DOI: 10.1186/s10086-019-1843-z

Article submitted: December 13, 2021; Peer review completed: March 20, 2022; Revised version received and accepted: March 25, 2022; Published: March 29, 2022.
DOI: 10.15376/biores.17.2.2780-2809